1993

Reduction of polyatomic ion interferences in inductively coupled plasma mass spectrometry with cryogenic desolvation

Luís Cláudio Alves
Iowa State University

INFORMATION TO USERS

This manuscript has been reproduced from the microfilm master. UMI films the text directly from the original or copy submitted. Thus, some thesis and dissertation copies are in typewriter face, while others may be from any type of computer printer.

The quality of this reproduction is dependent upon the quality of the copy submitted. Broken or indistinct print, colored or poor quality illustrations and photographs, print bleedthrough, substandard margins, and improper alignment can adversely affect reproduction.

In the unlikely event that the author did not send UMI a complete manuscript and there are missing pages, these will be noted. Also, if unauthorized copyright material had to be removed, a note will indicate the deletion.

Oversize materials (e.g., maps, drawings, charts) are reproduced by sectioning the original, beginning at the upper left-hand corner and continuing from left to right in equal sections with small overlaps. Each original is also photographed in one exposure and is included in reduced form at the back of the book.

Photographs included in the original manuscript have been reproduced xerographically in this copy. Higher quality 6" x 9" black and white photographic prints are available for any photographs or illustrations appearing in this copy for an additional charge. Contact UMI directly to order.

U·M·I

University Microfilms International
A Bell & Howell Information Company
300 North Zeeb Road. Ann Arbor, MI 48106-1346 USA
313/761-4700 800/521-0600

Order Number 9405046

Reduction of polyatomic ion interferences in inductively coupled plasma mass spectrometry with cryogenic desolvation

Alves, Luís Cláudio, Ph.D.

Iowa State University, 1993

U·M·I
300 N. Zeeb Rd.
Ann Arbor, MI 48106

Reduction of polyatomic ion interferences in inductively coupled plasma mass spectrometry with cryogenic desolvation

by

Luís Cláudio Alves

A Dissertation Submitted to the
Graduate Faculty in Partial Fulfillment of the
Requirements for the Degree of
DOCTOR OF PHILOSOPHY

Department: Chemistry
Major: Analytical Chemistry

Approved:

Signature was redacted for privacy.

In Charge of Major Work

Signature was redacted for privacy.

For the Major Department

Signature was redacted for privacy.

For the Graduate College

Iowa State University
Ames, Iowa

1993

To my Mother

For all her sacrifice for my success

TABLE OF CONTENTS

GENERAL INTRODUCTION

Since the first prototype by Houk and co-workers (1–7), inductively coupled plasma mass spectrometry (ICP-MS) has expanded and matured rapidly. ICP-MS has developed into a highly competitive analytical technique for routine trace analysis and instruments are now sold by manufacturers worldwide. There have been numerous reviews and general studies of ICP-MS (8–13). There are four chief alluring characteristics of ICP-MS. The excellent detection limits (0.1 – 10 ppt), comparable to or better than those obtained with electrothermal vaporization atomic absorption spectrometry (ETV-AAS), multiple element analysis, fast isotope ratio capability, and very simple and unique mass spectra, make ICP-MS an extremely attractive analytical tool. The simplicity of elemental mass spectra relative to the atomic emission spectra (AES) of the elements is an important advantage of ICP-MS over ICP-AES.

Although not as widespread as in ICP-AES, some severe interferences exist in ICP-MS. These phenomena are generally the deciding factors in the success (or lack thereof) of ICP-MS for a particular application. There are two general groups of interferences: spectroscopic overlap and non-spectroscopic or matrix interferences. The non-spectroscopic interferences (matrix effects) can be further subdivided into (a) suppression and enhancement effects and (b) changes in size of sampler and skimmer orifices caused by solutes present in the sample.

The sample matrix, in addition to introducing background spectral features, also may induce changes in the analyte signal intensity (14–18). Generally, the matrix effect can be associated with changes in transmission through the ion optics preceding the mass spectrometer. High ion currents caused by the high

concentration of the concomitant defocus the ion optics via space charge effects (19). In general, the lower the atomic mass of the analyte, the greater is the effect of a given added concomitant or matrix element on the ion count rate of the analyte. For a given analyte, the greater the atomic mass and degree of ionization of the interfering element, the greater is the effect of the matrix element on the analyte count rate. Finally, the extent of the matrix effect depends on the absolute amount of the matrix element present, not on the relative amount of the matrix element to analyte (20).

If the amount of total dissolved solids in a liquid sample is also high (above 1%), solute condenses on the relatively cool sampling and skimmer cone, which blocks the cone orifices. This blocking gives rise to an erratic loss of signal, poor precision, and a considerable signal drift over short periods of time (21).

If necessary, a number of methods can be used to overcome some of the non-spectroscopic interference effects. Special operating conditions (22–26), flow injection (26–28), dilution of samples (20, 24, 29, 30), internal standards or isotope dilution (14, 16, 17, 24, 31–34), matrix matching (35, 36), and standard addition (37) can all be used to cope with such effects. The most satisfactory method for some matrices, however, may be to separate the analytes from the matrix using techniques such as ion exchange separation or co-precipitation (38–44). In this case the matrix can be totally removed with the additional benefit of analyte pre-concentration.

Several specific spectroscopic sources of interferences can be identified in ICP-MS and these include basic background species, interelement spectral overlaps, and polyatomic ions containing matrix elements. The fundamental background species in ICP-MS consist of species that originate from argon, air, and water when

aqueous samples are nebulized into an Ar ICP. The major species include O^+, N_2^+, NO^+, O_2^+, Ar^+, ArH^+, ArO^+, and Ar_2^+. Some of the more evident and severe spectral overlap problems include $^{28}Si^+$ (N_2^+), $^{31}P^+$ (NOH^+), $^{32}S^+$ (O_2^+), $^{40}Ca^+$ (Ar^+), $^{56}Fe^+$ (ArO^+), and $^{80}Se^+$ (Ar_2^+). For each of these elements, alternative isotopes are available, which can be used at the expense of sensitivity.

The nature of the sample matrix may add considerable complexity to the background spectrum. The major elements present in the solvents or acids used during sample preparation (e.g., N, Cl, and S) combine with each other and with Ar, H, and O. The polyatomic ion interferences characteristic of different acid media are known, and the major ions of interest have been recognized and tabulated (1, 4, 9, 45–48). Some of the more evident and severe spectral overlap problems from matrix elements include $^{51}V^+$ ($^{35}Cl^{16}O^+$) and $^{75}As^+$ ($^{40}Ar^{35}Cl^+$).

Interelement spectral overlaps are observed between different atomic ions with the same nominal mass. In reality, the isotope masses may differ by a small amount which cannot be resolved by the quadrupole mass analyzer used in commercial ICP-MS systems. Because interelement overlaps are predictable and natural abundance values are tabulated, schemes can be developed to correct for the occurrence of interelement spectral overlaps. However, such correction procedures can run into considerable difficulty if other concomitant background species are not carefully considered. For example, the correction of the $^{58}Ni^+$ signal for the presence of Fe ($^{58}Fe^+$) consists of measuring the signal at mass 56 and, assuming it to come completely from $^{56}Fe^+$, subtracting 0.0036 times that measured count from the count at mass 58. This procedure corrects for the contribution of $^{58}Fe^+$ to the total count rate at m/z = 58. However, the signal at mass 56 also has a major

contribution due to $^{40}Ar^{16}O^+$, and depending on the actual relative and absolute amounts of Ni and Fe present, a serious error could result.

The most serious general class of spectral interference problem is that involving oxide and hydroxide species (29, 45, 49–52). Oxide ions may be formed from the plasma gases, air entrainment, the sample solvent, and the matrix and analyte components of the sample. Almost all analyte and matrix elements form monoxide (MO^+) and hydroxide (MOH^+) ions to some extent. The most serious MO^+ interferences are from elements that form refractory oxides, particularly the light rare earths, W, Mo, etc. Table 1 presents a list of potential interferences in Ni determinations and the Appendix shows a more thorough listing of potential interferences from $m/z = 1$ to 254. Several means of correcting the MO^+ contribution have been described (17, 29, 39, 50, 53–55). Operating conditions such as aerosol gas flow rate, forward power, and sampling position can be found that alleviate these interferences (45, 46, 51, 56–62). However, these adjustments generally jeopardize the analyte sensitivity and tend to work best if the amount of MO^+ is previously minimized. A great deal of research in ICP-MS has focused on ways to reduce or cope with oxides.

ICP-AES and ICP-MS have been used for the determination of trace metals in some organic solvents (63–67). Typical applications have included the determination of trace metals in lubricating oils (68), crude oils (69), and the usual organic:aqueous eluents used in high-performance liquid chromatography (HPLC) (70). However, present techniques often give rise to operating difficulties, and a number of more fundamental studies have identified a range of potential problems associated with the introduction of organic solvents into the plasma (67, 71, 72). These problems include deposition of carbon on the torch and sampling cones of the

Table 1. Potential Interferences in the Mass Region for Nickel Determinations by ICP-MS

m/z	Element[a]	Interferences
58	Ni(67.77), Fe(0.33)	^{42}CaO, NaCl
60	Ni(26.16)	$^{43}CaOH$, ^{44}CaO
61	Ni(1.25)	$^{44}CaOH$
62	Ni(3.66)	^{46}CaO, Na_2O, NaK
64	Ni(1.16), Zn(48.89)	$^{32}SO_2$, $^{32}S_2$, ^{48}CaO

[a] Percentage natural abundance in parentheses.

ICP mass spectrometer and a decrease in plasma stability. Carbon, derived largely from the solvents, condenses on the relatively cool metal surfaces of the sampler, skimmer, and the mass spectrometer lens surfaces, which leads to a rapid loss of sensitivity. Volatile organic solvents cause instability in the ICP due to extremely high solvent transport efficiency in the introduction system and excessive solvent loading of the plasma (73). In order to alleviate many of these difficulties, cooled spray chambers (63, 64, 71, 72), a reduction in sample uptake rates (66, 67), increased forward power (64), and the addition of a small flow of oxygen (~ 2%) into the nebulizer gas to minimize carbon deposition (64), have been suggested.

The application of desolvation procedures for removal of solvent prior to the ICP has been examined by several workers including Maessen (71, 72, 74, 75), Hausler (76–78), Boorn (67), and Ebdon (63, 79, 80). Reduction of solvent vapor loading in plasmas can be experimentally accomplished by lowering the liquid uptake rate and aerosol carrier gas flow, or by cooling the aerosol stream. Previous investigators however, have not achieved the level of solvent removal that this work (81, 82, 83) does because of two main reasons: first and foremost, this work uses repetitive heating and cooling steps and second, temperatures as low as -80°C are used. No one else have applied repetitive desolvation and the lowest temperature used up until this work was - 50°C by Maessen and co-workers (71). Maessen concluded that saturated solvent vapor may condense back onto the aerosol particles but wrongly inferred that only a limited reduction in the solvent plasma load was achievable by aerosol cooling. Moreover, Maessen erroneously concluded that more analyte was trapped with decreasing condenser temperature. Different condenser configurations have emerged and for example, Ebdon and co-workers (80) have used Peltier coolers which are cooled by water flowing over copper plates.

They could not cool the aerosol below -40°C, but noted the probable advantages of removing more solvent by cooling the aerosol at still lower temperatures. This present work shows a rather thorough solvent removal by multiple cryogenic desolvation steps. The analyte sensitivity and detection limit with cryogenic desolvation are comparable or superior to the ones obtained when aqueous samples are nebulized and only regular desolvation is used.

Overview of Dissertation

The purpose of this dissertation is to describe how cryogenic desolvation can be applied to lessen the polyatomic ion interferences in inductively coupled plasma mass spectrometry (ICP-MS). This dissertation is presented as three complete scientific manuscripts with accompanying tables, figures, and literature cited. Additional literature cited in this general introduction and in the summary following the last paper will be given after the summary.

The first paper (81) outlines the apparatus and scheme used in the cryogenic desolvation of aqueous aerosols. A continuous-flow ultrasonic nebulizer generates the aerosol which passes through a regular desolvation step. The aerosol is then sent to a system that contains cooling (-80°C) and heating (+140°C) steps to freeze out the remaining water. Polyatomic ions such as ArO^+, $ArCl^+$, ClO^+, and MO^+ (metal oxides) are greatly suppressed. Comparisons are made between cryogenic and other desolvation methods.

The second paper (82) describes improvements in the cryogenic desolvation method as well as its application to real samples such as seawater and urine reference materials. A mixed gas plasma containing a small percentage of H_2 to the central channel improves the sensitivity obtained with cryogenic desolvation.

The third paper (83) reports the cryogenic desolvation of several organic solvents with ICP-MS. Metal standards in pure organic solvents are continuously nebulized with an ultrasonic nebulizer. The plasma exhibits green C_2 band emission when ethanol and acetone are used but no green emission is observed when methanol and acetonitrile are nebulized. The amount of carbon deposition on the sampler cone depends on the solvent used and the carbon is easily burned off of the sampler cone by the addition of O_2 to the central channel. Moreover, the analyte sensitivities were compared in both methanol and water standards and found to be comparable to each other and to the sensitivities obtained with aqueous samples in the presence of regular desolvation only. Volatile and low melting point organometallic compounds were dissolved in methanol and nebulized. The metal sensitivities were comparable or slightly superior to the metal sensitivities in nitrate salts. However, substantial memory effects were observed and these varied among the organometallic compounds tested between 2 and 0.2% of the steady state signal.

PAPER I.

REDUCTION OF POLYATOMIC ION INTERFERENCES IN INDUCTIVELY COUPLED PLASMA MASS SPECTROMETRY BY CRYOGENIC DESOLVATION

ABSTRACT

Multiple desolvation steps at -80°C for a continuous-flow ultrasonic nebulizer reduced the load of water and HCl on an argon inductively coupled plasma (ICP). Consequently, the oxide ratios MO^+/M^+ for Ca, Mo, and La were 0.02% - 0.05%. Polyatomic ion interferences from ArO^+, ClO^+, and $ArCl^+$ were also reduced by several orders of magnitude. Measured isotope ratios for Ni, Cd, and Fe were in good agreement with accepted natural values, and the detection limits were 2-20 ng L^{-1} for Ni, Fe, V, As, and Cd in the presence of concentrated matrices of HCl, Ca, or Mo that would normally cause polyatomic ion interference. Eight additional seconds were necessary for sample rinse-out and analyte sensitivity was reduced by a factor of two when cryogenic desolvation was used. UO^+/U^+ ratios were reduced to 0.06% when cryogenic desolvation was used and acetylene was added to the central channel. Sodium matrices up to 100 mg L^{-1} decreased the La^+ count rate but did not affect the oxide ratio LaO^+/La^+. At 1000 mg L^{-1} NaCl the LaO^+/La^+ ratio increased to 0.08%.

INTRODUCTION

Inductively coupled plasma mass spectrometry (ICP-MS) has become an important technique for trace elemental analysis of solutions. Reasons for this include low detection limits (1-10 ng L^{-1}), the ability to monitor stable isotope ratios, and the simplicity of the spectra relative to those seen in ICP emission spectrometry. Nonetheless, spectral overlap does hamper the determination of some important elements by ICP-MS. Most of the serious overlaps involve polyatomic ions that incorporate oxygen and, in general, it is desirable to attenuate these species as much as possible. Houk *et al.* originally identified most of these major spectral overlaps (1, 2) and Horlick and co-workers have compiled extensive tables of spectral interferences for ICP-MS (3, 4).

Reasonable corrections for overlap interferences are sometimes possible. Many investigators have attempted to reduce the level of the oxygen-containing interferences or have devised ways to cope with them. The tactics chosen to prevent interference from oxide ions vary widely. McLaren *et al.* (5, 6) and Lam and Horlick (7) used a mixed gas N_2-Ar ICP, which attenuated ArO^+ substantially and reduced metal oxide levels to some extent. Jarvis, Gray, and McCurdy measured Eu^{2+} to avoid overlap with BaO^+ (8) and Vaughan and Templeton applied principal component analysis for the determination of nickel isotopes in the presence of calcium (9).

Other work has focused on removal of water from the ICP, which decreases the amount of oxygen present. A cooled spray chamber or a condenser to remove solvent vapor has been widely used (10-19). Desolvation with a heater and condenser (1, 5, 20) and various types of solvent separators (6, 17, 21-25) have been

used for this purpose. Dry sample introduction methods include electrothermal vaporization (26), arc nebulization (27), and laser ablation (28).

Cryogenic desolvation has been previously employed by Wiederin *et al.* for the analysis of organic solvents by ICP atomic emission spectrometry (AES) (29). The present paper describes the use of multiple cryogenic desolvation steps for the reduction of polyatomic ion levels in ICP-MS via reduction of the water vapor load. Spectral interferences caused by ArO^+ on Fe^+, by CaO^+ on Ni^+, by MoO^+ on Cd^+, by ClO^+ on V^+, and by $ArCl^+$ on As^+ are reduced substantially. Cryogenic desolvation with 0.1% acetylene in the aerosol gas flow reduced UO^+/U^+ to 0.06%.

EXPERIMENTAL SECTION

Instrumentation

A Perkin-Elmer Sciex ELAN Model 250 ICP mass spectrometer with upgraded ion optics was used. Unless otherwise stated, the operating conditions given in Table 1 were employed. Figure 1 shows the sample nebulization and desolvation scheme used. Samples were introduced to the ultrasonic nebulizer by a peristaltic pump (Rainin Miniplus-2 Instrument Co., Woburn, MA). The aerosol gas flow rate was generally about 1.8 L min^{-1} and was adjusted to give the maximum M^+ signal obtainable. The need for a high aerosol gas flow rate agreed with Lam and McLaren's observation that as the water vapor load decreased, the analyte count rate maximized at higher aerosol gas flow rate (5).

Desolvation Procedures

The aerosol generated by the ultrasonic nebulizer (Figure 1) was heated to 140°C and then passed through a series of condensers. The first condenser at 0°C removed most of the water present. The partially dried aerosol stream was warmed to room temperature before it entered a second glass condenser at -80°C (Figure 2). This second condenser had a wide flow passage (~ 1 cm gap between inner and outer wall), which could accommodate a substantial layer of ice without blocking. The aerosol stream then went to a set of copper loops where it was repeatedly cooled and heated at -80°C and 140°C respectively. Tygon tubing was used to transport the aerosol from the heating/cooling loops to the ICP.

Table 1. Operating conditions

ICP torch	Ames Laboratory design (30); outer tube extended 30 mm from inner tubes
Plasma forward power	1.25 kW
Argon flow rates (L min^{-1})	
Outer	12
Auxiliary	0.4
Aerosol	1.8
Sampling position	20 mm above load coil, on center
Sampler	Copper, 1.1 mm diam. orifice
Skimmer	Nickel, 0.9 mm diam. orifice
Ion lens settings	
Bessel box stop	- 5.9 V
Bessel box barrel	+ 5.4 V
Bessel box plate	- 11.0 V
Einzel 1 and 3	- 19.8 V
Einzel 2	- 130.0 V
Electron multiplier voltage	- 4000 V
Ultrasonic Nebulizer	Cetac Technologies (Omaha, NE) Model U-5000 current setting = 6 (arbitrary units) desolvation heater temp. = 140°C desolvation condenser temp. = 0°C
Cryocooler	Cryocool CC-100II at - 80°C Neslab (Portsmouth, NH)

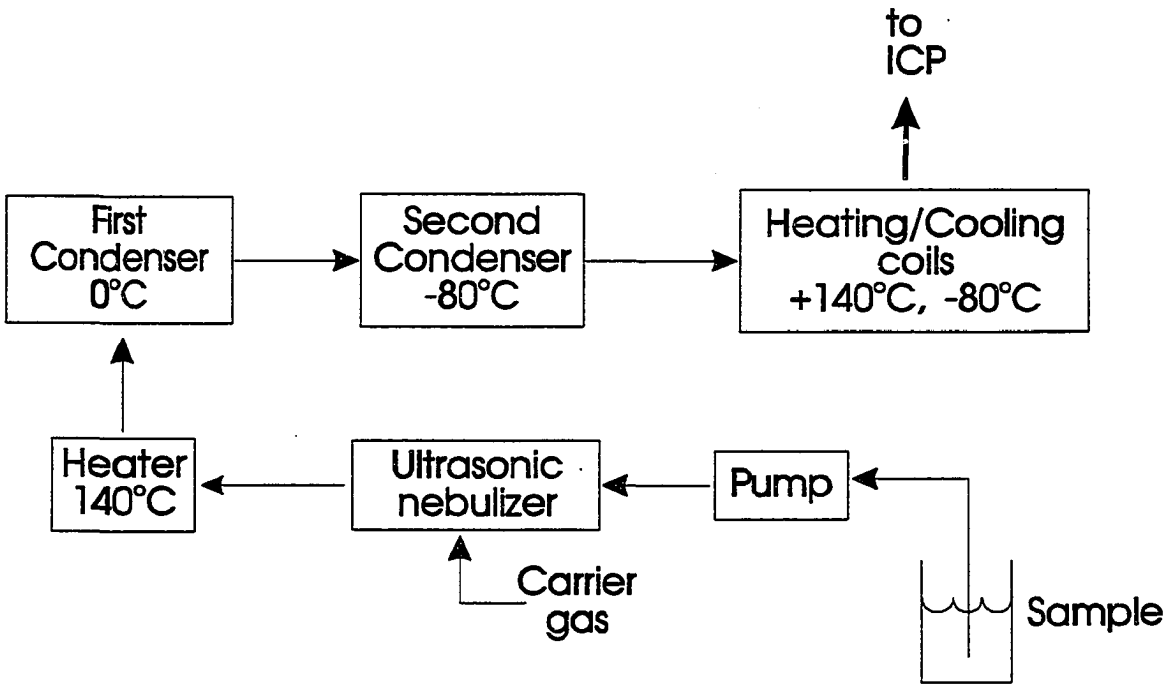

Figure 1. Nebulization and desolvation scheme.

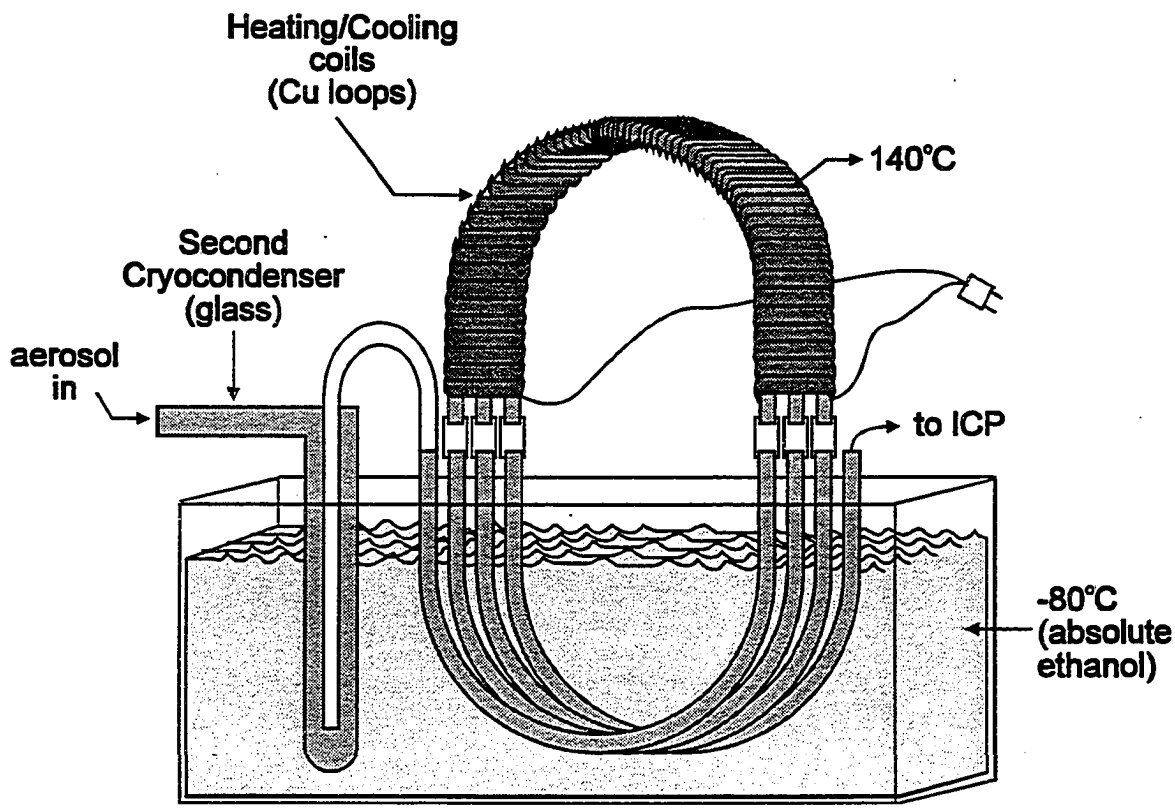

Figure 2. Multiple cryogenic desolvation system.

The heating/cooling loops (Figure 2) were made up of seven U-shaped tubes each 10 mm i.d. x 13 mm o.d. x 0.5 m long of soft copper tubing. The four lower U-tubes were placed in the cryocooler at -80°C and the three upper U-tubes were heated electrically to a surface temperature of 140°C. These U-tubes were interconnected with lengths of polyethylene tubing to reduce the thermal conduction between hot and cold tubes. Copper was used because of its high thermal conductivity.

The condensers did not plug during eight hours of continuous operation with the arrangement shown in Figure 2. The deposited ice was easily removed by simply removing the second and third condensers from the bath for a few minutes. The ICP could be kept on during this warming process. If the second condenser, with its wide gap, was omitted, the narrower copper loops froze shut with ice in only ~ 1 hour.

Data Acquisition

Data were acquired in the multielement mode at low resolution setting (1 amu width at base of peak) with 3 measurements per peak, 20 ms dwell time, and 1 s measurement time. The measurement time was reduced to 0.5 s during rinse-out studies. Spectra were acquired in the sequential mode with 10 measurements per peak and a 1 s measurement time. Count rates were uncorrected for isotopic overlaps unless otherwise stated. Detection limits were calculated as the analyte concentrations necessary to yield net signals equivalent to three times the standard deviation of twenty measurements of the background.

Standard Solutions

Standard solutions were prepared from 1000 mg L^{-1} standards from Fisher Scientific (Fair Lawn, NJ) with a 1% nitric acid solution (Ultrex II Ultrapure reagent grade, J. T. Baker, Phillipsburgh, NJ). The hydrochloric acid used was also Ultrex II. Distilled deionized water was obtained from a Barnstead Nanopure-II system (18 MW, Barnstead Co., Newton, MA). Solutions containing sodium were prepared from a reagent grade stock solution of NaCl at 10 g L^{-1}.

RESULTS AND DISCUSSION

Desolvation and Plasma Characteristics

The aerosol stream leaving the spray chamber of the nebulizer contained water as both liquid aerosol droplets and water vapor. Since water was the major source of oxygen in the plasma when nebulizing aqueous samples, decreasing water loading decreased the oxygen concentration in the plasma. Oxygen in the plasma also originated from oxygen-containing analyte, oxygen-containing gases in the argon supply, and air entrainment.

Most of the water vapor present in the aerosol stream leaving the first condenser at 0°C froze on the first two inches of the second condenser (Figure 2). Some fine droplets were seen at the exit port of the second condenser. Thus, water vapor in the second condenser also deposited onto the analyte particles, as seen previously with organic solvents (29). Because of this recondensation phenomenon and the plugging problem described in the previous section, the simple cryocondenser (i.e., just cold glass loops) described previously (29) for removing organic solvents was not consistently effective for removing water.

An experiment was performed to ascertain how many heating and cooling cycles were necessary in the copper heating/cooling loops to remove the water that deposited back onto the particles. The desolvation system was operated for eight hours and the amount of water frozen in each tube was measured. Three warm U-tubes on the top and four cold U-tubes on the bottom was the optimum arrangement to remove water while minimizing rinse-out times and retaining useful analyte signal.

No special conditions were required to ignite or sustain the plasma. Visual observation of the plasma showed that the central channel was narrower when cryogenic desolvation was employed.

Background Mass Spectra and Removal of ClO^+, $ArCl^+$, and ArO^+

A drawback of using Cu tubes is evident when nebulizing water (Figure 3). The 50-fold increase in the count rates already observed at *m/z* 63 and 65 is presumably from some Cu from the tubes reaching the plasma. Copper tubing with an inner surface of a thin layer of an inert metal might prevent the increase in the background count rates at these masses.

The major isotopes of iron ($^{56}Fe^+$ and $^{54}Fe^+$) are usually obscured by ArO^+ and ArN^+, respectively. An average background count rate of 12500 counts s^{-1} was obtained at *m/z* 56 when the aerosol was desolvated only by conventional means, i.e., cooling at ~ 0°C (Figure 3a). The average count rate at *m/z* 56 was reduced to 330 counts s^{-1} when cryogenic desolvation was used (Figure 3b), which corresponded to a reduction factor of about 36 for ArO^+. Unfortunately, the count rate for ArN^+ was enhanced by a factor of two with cryogenic desolvation. Presumably, N_2 or other impurity gases containing N were not removed in the cryogenic loops, hence ions containing N remained in the spectra. The reasons for the increase in the count rate for ArN^+ during cryogenic desolvation are not clear. Perhaps extensive removal of water from the plasma caused a modest increase in temperature. Due to the high ionization energy of N (14 eV), such a temperature increase caused a large relative increase in the density of N^+. The ArN^+ may then have been formed from collisions of N^+ with Ar during the extraction process.

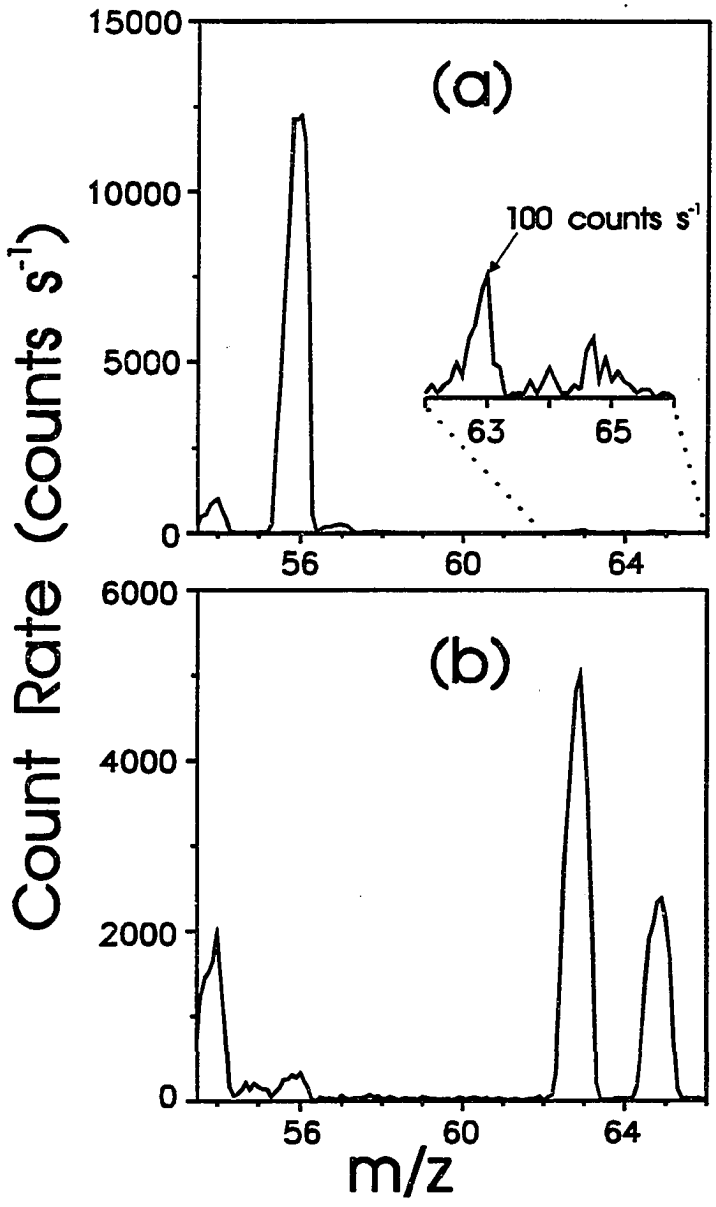

Figure 3. Background mass spectra for water (a) without cryogenic desolvation and (b) with cryogenic desolvation. Note that the vertical scale is expanded in (b).

A solution of 100 μg L^{-1} Fe in 1% HNO_3 solution was nebulized. Table 2 lists the Fe isotope ratios found. Apart from ratios involving ^{58}Fe, the other Fe isotope ratios are in reasonable agreement with the expected natural values. Table 3 shows the sensitivities and detection limits obtained for Fe isotopes.

Chlorine oxide ($^{35}ClO^+$) overlaps the major isotope of vanadium (^{51}V, 99.75% natural abundance) and $^{40}Ar^{35}Cl^+$ obscures the only stable isotope of As. Thus, the determination of V and As in HCl solutions is difficult. Background spectra obtained when 1% HCl solutions were nebulized with or without cryogenic desolvation are shown in Figure 4. With conventional desolvation (Figure 4a), the peak for $^{35}Cl^+$ is over 2 x 10^6 counts s^{-1}. With cryogenic desolvation (Figure 4d), the peak for $^{35}Cl^+$ is only ~ 2500 counts s^{-1}. Apparently, cryogenic desolvation reduces the amount of chlorine reaching the plasma, presumably by condensing most of the HCl. Consequently, the count rates at *m/z* 51 and 53 (ClO^+) and 75 ($ArCl^+$) are also reduced. Figures 4d and 4e compare the count rates for ClO^+ and Figures 4c and 4f compare the count rates for $ArCl^+$ with and without cryogenic desolvation. The count rates observed for $ArCl^+$ (*m/z* =75 and 77) in Figure 4f are indistinguishable from the usual background count rate seen with this particular nebulizer and ICP-MS instrument. The sensitivities and detection limits obtained for As and V in 1% HCl are given in Table 3. The interferences from chlorine-containing ions are dramatically lessened; therefore, cryogenic desolvation allows for very good detection limits for V and As in spite of the high concentration of HCl.

Table 2. Iron isotope ratios with cryogenic desolvation[a]

Isotope Ratio	Measured Ratio	Measured ratio / Natural ratio	RSD (%)[b]
54/56	0.068	1.032	0.8
54/57	2.796	1.062	1.1
54/58	4.554	0.781	2.0
56/57	41.322	0.972	0.8
56/58	67.568	1.309	1.8
57/58	1.629	1.356	1.8

[a] The sample was 100 μg L^{-1} Fe in 1% HNO_3, which yielded 900,000 counts s^{-1} for $^{56}Fe^{+}$.

[b] RSD of 20 consecutive measurements of indicated isotope ratio.

Table 3. Sensitivities and detection limits obtained with cryogenic desolvation

Element	*m/z*	Sensitivity counts s^{-1} ppm^{-1}(x 10^6)	Detection Limit (ng L^{-1})
V[a]	51	6	2
Fe[b]	54	0.6	50
	56	9	4
	57	0.2	50
	58	0.04	1300
Ni[c]	58	6	3
	60	3	5
	61	0.1	90
	62	0.3	30
	64	0.2	100
As[d]	75	2	5
Cd[e]	106	0.03	300
	108	0.02	700
	110	0.3	40
	112	0.6	30
	114	0.7	20
	116	0.2	80

[a] 200 µg L^{-1} V in 1% HCl

[b] 100 µg L^{-1} Fe in 1% HNO_3

[c] 50 µg L^{-1} Ni in 100 mg L^{-1} Ca

[d] 1 mg L^{-1} As in 1% HCl

[e] 200 µg L^{-1} Cd in 100 mg L^{-1} Mo

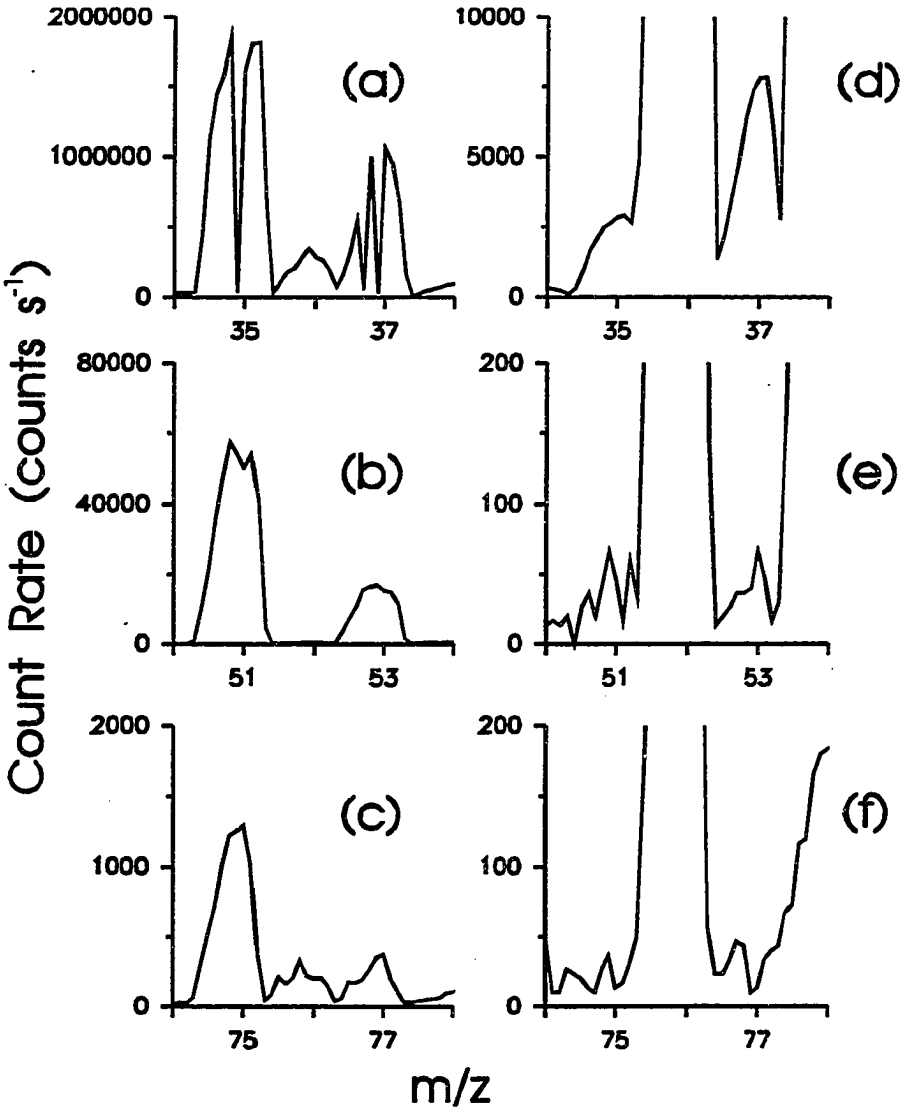

Figure 4. Background mass spectra for 1% HCl. (a), (b), and (c) without cryogenic desolvation and (d), (e), and (f) with cryogenic desolvation. Note the changes in the vertical and horizontal scales. Split peaks for Cl^+ in (a) are merely due to counting loss.

Removal of Metal Oxides

The ability of cryogenic desolvation to remove metal oxide ions was studied with solutions of Ca (100 mg L^{-1}), Mo (1 mg L^{-1}), and La (100 µg L^{-1}) in 1% HNO_3. When cryogenic desolvation was used, the count rate ratios for $^{43}CaO^+/^{43}Ca^+$ and $^{139}LaO^+/^{139}La^+$ were ~ 0.05%, and the ratio for $^{98}MoO^+/^{98}Mo^+$ was ~ 0.02%. These MO^+/M^+ ratios are at least 10 times better than can be obtained with a cooled spray chamber under plasma operating conditions that yield the maximum analyte count rate. Our MO^+/M^+ ratios are similar to those obtained with sample introduction methods such as laser ablation or electrothermal vaporization (31) that are completely dry.

Molybdenum oxide ions overlap all the major isotopes of Cd, which complicates measurement of Cd in a Mo matrix by ICP-MS (32). Table 4 shows the isotope ratios obtained for Cd at 200 µg L^{-1} in 100 mg L^{-1} Mo. Apart from ^{116}Cd ratios, all the other Cd isotope ratios were in very good agreement with the natural values expected, despite the 500-fold excess of Mo. Table 3 shows the sensitivities and detection limits obtained for Cd with this Mo matrix present.

Another example of the potential value of cryogenic desolvation is found in the determination of trace levels of Ni in samples with high Ca levels such as human serum, urine, and fresh water (9, 33). Nickel measurement is hampered by the formation of CaO^+ and $CaOH^+$ species that overlap all the Ni isotopes. Although correction procedures based on principal component analysis have been developed to correct for interferences from CaO^+ and $CaOH^+$ (9), it is obviously desirable to attenuate these ions. A solution containing 50 µg L^{-1} Ni and 100 mg L^{-1} Ca in 1% HNO_3 was nebulized. Table 5 presents the results obtained for Ni isotope ratios and compares them to the expected natural values. Apart from ratios

Table 4. Cadmium isotope ratios with cryogenic desolvation[a]

Isotope Ratio	Measured Ratio	Measured ratio / Natural ratio	RSD (%)[b]
110/111	0.954	0.9765	0.7
110/112	0.499	0.9632	0.6
110/114	0.406	0.9325	0.4
110/116	0.894	0.5335	0.9
111/112	0.524	0.9863	0.7
111/114	0.426	0.9551	0.7
111/116	0.937	0.5464	0.8
112/114	0.814	0.9682	0.4
112/116	1.789	0.5540	0.8
114/116	1.847	0.4803	0.8

[a] Background subtracted for isotope 116 only. The sample was 200 $\mu g\ L^{-1}$ Cd in 100 $mg\ L^{-1}$ Mo, which yielded 138200 counts s^{-1} for ^{114}Cd.

[b] RSD of 20 consecutive measurements of indicated isotope ratio.

Table 5. Nickel isotope ratios with cryogenic desolvation[a]

Isotope Ratio	Measured Ratio	Measured ratio / Natural ratio	RSD (%)[b]
58/60	2.565	0.975	0.5
58/61	58.824	0.939	1.9
58/62	18.182	0.962	1.1
58/64	61.350	0.445	1.5
60/61	22.936	0.963	1.8
60/62	7.107	0.986	1.1
60/64	23.923	0.456	1.5
61/62	0.310	1.024	2.0
61/64	1.043	0.474	2.1
62/64	3.365	0.463	1.4

[a] Background subtracted for isotopes 61 and 64 only. The sample was 50 $\mu g\ L^{-1}$ Ni in 100 $mg\ L^{-1}$ Ca, which yielded 319000 counts s^{-1} for ^{58}Ni.

[b] RSD of 20 consecutive measurements of indicated isotope ratio.

involving ^{64}Ni, all the other Ni isotope ratios were in very good agreement with the natural values expected. Table 3 presents a summary of the sensitivities and detection limits obtained for Ni isotopes in the presence of 100 mg L^{-1} Ca.

In general, the analyte sensitivities given in Table 3 are ~ 2 times lower than those obtained with this particular ultrasonic nebulizer and ICP-MS device when only conventional desolvation was employed. Perhaps some analyte was lost during cryogenic desolvation, or perhaps the yield of analyte ions is reduced when no water or other molecular gas is added to the ICP. Since the overlapping interferences were removed more extensively, there was an overall improvement in the detection limits with cryogenic desolvation for elements plagued by such interferences.

Removal of UO^+

The bond dissociation energy of UO^+ is very high (~ 8 eV) (34). Although spectral overlap from UO^+ is not normally an analytical problem, studies of this species were undertaken to evaluate the ability of cryogenic desolvation to attenuate even the most tenacious oxide ions. The UO^+/U^+ ratio was 1% when a solution of 100 μg L^{-1} U in 1% HNO_3 was nebulized even with cryogenic desolvation. This UO^+/U^+ ratio was reduced further when a 2% acetylene/argon mixture was added at 0.1 L min^{-1} to the aerosol gas. The total aerosol flow was 1.8 L min^{-1}, so the overall level of acetylene in the aerosol gas flow was ~ 0.1%. At this acetylene concentration the UO^+/U^+ ratio was reduced to 0.06% (Figure 5). This value of UO^+/U^+ is superior by a factor of 20-40 to the UO^+/U^+ ratios commonly obtained during nebulization of aqueous solutions (5).

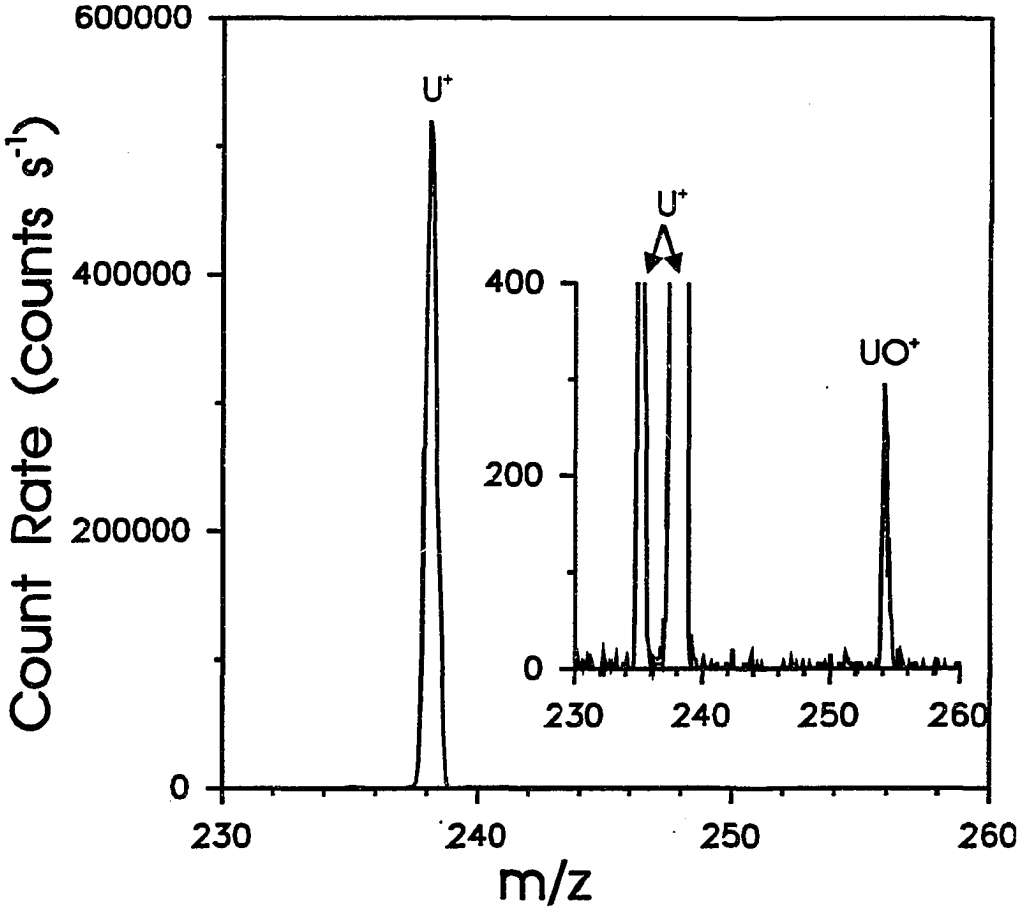

Figure 5. Mass spectrum for 100 μg L^{-1} U in 1% HNO_3 with cryogenic desolvation and 0.1% acetylene added to the aerosol gas. Note the absence of UC^+ at $m/z = 250$.

It is also instructive to compare the UO^+/U^+ ratio measured in the present work with that reported by McLaren *et al.* (6), who desolvated aqueous aerosols with a membrane separator and dry ice/acetone trap. They also added 4% N_2 into the outer gas to attenuate oxides further. Otherwise, the ICP-MS device used by them was from the same manufacturer and was of similar vintage as ours. McLaren *et al.* reported UO^+/U^+ ratios of ~ 0.1% to 0.2%, depending on the power and aerosol gas flow rate used (6). Our value of 0.06% for UO^+/U^+ is superior to that of McLaren *et al.* (6) by a factor of two to three and is comparable to the best UO^+/U^+ ratios achieved with "dry" sample introduction techniques such as laser ablation. Finally, uranium can form refractory carbides, but UC^+ was not seen in the present work (< 10 counts s^{-1}) even when a 100 mg L^{-1} U solution was nebulized in the presence of acetylene.

Acetylene may play a role similar to that suggested by McLaren *et al.* (6) for nitrogen added to the argon outer gas. The carbon from the dissociation of acetylene may compete with uranium for the oxygen remaining in the plasma. Signals for CO^+, CO_2^+, and $ArCO^+$ increased when acetylene was added, which supported this hypothesis. These results also agreed with McLaren's observation that reduction of water loading alone was not sufficient to attenuate UO^+/U^+ to levels appreciably below 1% (5, 6).

In this work, uranium was the only element tested that needed acetylene in the plasma to achieve low MO^+/M^+ ratios. For example, addition of acetylene did not improve LaO^+/La^+ ratios substantially. The drawbacks to adding acetylene are carbon deposition on the sampling cone and a reduction by a factor of 2 in the U^+ signal to 2×10^6 counts s^{-1} ppm^{-1} U. The carbon deposition was easily removed from the cone by adding ~ 1% O_2 to the central channel of the plasma for a

few seconds. Naturally, the usual carbon-containing polyatomic ions, such as C_2^+ and ArC^+ were intensified when acetylene was added.

Rinse-out Times and Precision

Figure 6 compares the rinse out profiles obtained with and without cryogenic desolvation. A solution of 200 μg L^{-1} Co in 1% HNO_3 was used. The Co signal decreased to 0.1% of its steady state value in 59 s with cryogenic desolvation, which was only 8 s longer than the rinse out time required with only conventional desolvation. The count rates for Co shown in Figure 6 are higher for cryogenic desolvation only because the ICP-MS conditions (particularly the aerosol gas flow rate) were optimized to yield maximum Co^+ signal during cryogenic desolvation. Naturally, the same aerosol gas flow rate, power, etc., were no longer optimum when the cryogenic desolvation apparatus was removed. The precisions obtained (Tables 2, 4–6) when cryogenic desolvation was used were typical of those for this ICP-MS device with an ultrasonic nebulizer.

Effect of Na Matrix on LaO^+/La^+ Ratios

The objective of this experiment was to determine if a salt matrix hampered removal of water. Solutions of 100 μg L^{-1} La in 0, 1, 10, 100, and 1000 mg L^{-1} NaCl were used. Table 6 shows the count rates for La^+ and LaO^+ for the solutions nebulized as well as the ratios for LaO^+/La^+. These data indicate that NaCl particles for NaCl concentrations up to 100 mg L^{-1} did not carry water into the plasma. The oxide ratio did rise to 0.075% when the most concentrated matrix (1000 mg L^{-1} NaCl) was nebulized.

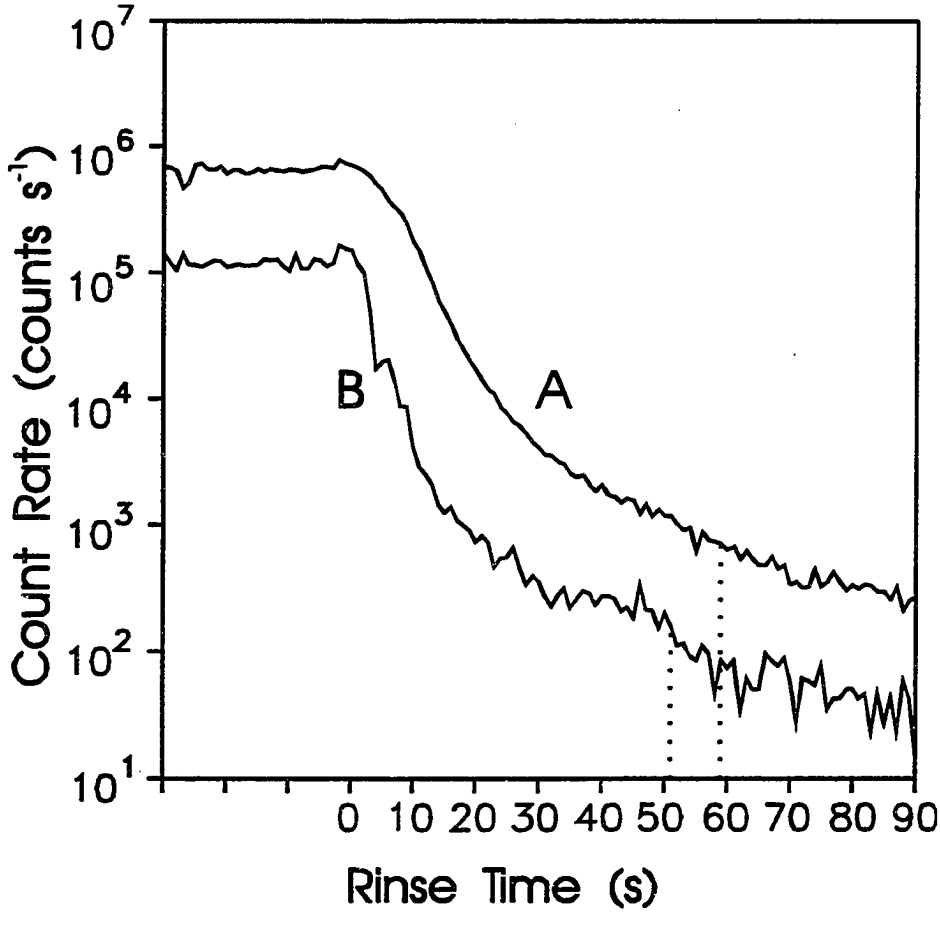

Figure 6. Comparison of rinse-out times obtained with an ultrasonic nebulizer and 200 μg L^{-1} Co solution with cryogenic desolvation (a) and with only conventional desolvation (b). The Co solution was replaced with distilled deionized water at time zero. Operating conditions were optimized to yield maximum Co^+ signal during cryogenic desolvation and kept constant thereafter.

Table 6. Matrix effect on La^+ count rate and LaO^+/La^+ ratios[a]

NaCl concentration (mg L^{-1})	La^+ count rate (counts s^{-1})	LaO^+ count rate (counts s^{-1})	LaO^+/La^+ (%)
0	773000	333	0.043
1	684000	303	0.044
10	621000	276	0.044
100	606000	322	0.053
1000	482000	362	0.075

[a] 100 μg L^{-1} La was present in all solutions. The RSD of La^+ signal was ~ 3% for 20 consecutive measurements.

Additional Observations

A 1% H_2SO_4 solution was also nebulized. The count rates for SO^+, SO_2^+, and SO_3^+ were not appreciably different from the levels obtained without cryogenic desolvation. Apparently, most of the H_2SO_4 was carried into the plasma by the aerosol. Temperatures above the boiling point of H_2SO_4 (330°C) (35) would be needed to vaporize the H_2SO_4 completely. In this work, such high temperatures were not used to avoid thermal overloading of the cryocooler bath. In general, oxygen that is chemically bound in ions in the solution will not be removed by cryogenic desolvation, unless the species containing the oxygen can be volatilized by the heater and then removed by the condenser.

The MO^+/M^+ ratios obtained with cryogenic desolvation varied from day to day but ratios of 0.05% or better were always attainable for LaO^+/La^+. The variation observed was probably primarily due to different concentrations of oxygen-containing impurities in the argon supplies used. The oxygen impurities in the argon supply became a concern when the solvent loading was reduced dramatically. Flushing the gas lines with a slow flow of argon when connecting new cylinders to the manifold improved the day-to-day consistency of the oxide ratios, presumably by preventing inclusion of air in the gas lines.

The isotope ratios involving the heaviest isotopes ($^{58}Fe^+$, $^{116}Cd^+$, and $^{64}Ni^+$) were the ones most distant from the expected natural values. These three isotopes were the last ones measured during each data acquisition cycle. Since isotopic overlaps at those *m/z* values were attenuated drastically, other factors not clear at this time, must have caused the errors observed. Interfering peaks from isotopes of possible impurity elements such as Ni (on ^{58}Fe), Sn (on ^{116}Cd), and Zn (on ^{64}Ni) were not seen in scans of these spectral regions.

CONCLUSION

A multiple cryogenic desolvation system for ICP-MS reduces MO^+/M^+ ratios to 0.05% for refractory elements including uranium while still maintaining good analyte sensitivity. This system can also reduce count rates for ArO^+, $ArCl^+$, ClO^+, and Cl^+ and can provide reasonable accuracy for Ni isotope ratios in the presence of a Ca matrix and Cd isotope ratios in the presence of a Mo matrix.

Introduction of organic solvents to the ICP by cryogenic desolvation of the aerosol has already been applied with atomic emission spectroscopy (29). This method should also prove useful to eliminate most of the organic solvent vapors when nebulizing non-aqueous samples in ICP-MS. Cryogenic desolvation with organic solvents is easier since the tubing does not clog and the temperature required to volatilize most organic solvents (e.g., methanol or acetone) is lower than that for aqueous solvents.

The water load to the plasma could theoretically be reduced further if lower temperatures were used. The freezing point of argon is likely the lower temperature limit for cryogenic desolvation with an Ar ICP. The use of acetylene and other reagents to chemically tailor the plasma warrants further studies.

ACKNOWLEDGMENTS

The authors appreciate the contributions of Fred Smith and Robert Neddersen throughout this work. The loan of an ultrasonic nebulizer from Cetac Technologies, Inc., is gratefully acknowledged.

CREDIT

Ames Laboratory is operated by Iowa State University for the U. S. Department of Energy under Contract No. W-7405-Eng-82. Daniel R. Wiederin was supported by a Procter and Gamble Graduate Research Fellowship. This research was supported by the Office of Basic Energy Sciences, Division of Chemical Sciences.

SAFETY NOTE

Perchlorate solutions were not tested with cryogenic desolvation for fear of explosion upon heating. Extreme caution should be observed if the techniques described in this paper are applied to perchlorate solutions or solutions of other thermally unstable compounds.

LITERATURE CITED

(1) Houk, R. S.; Fassel, V. A.; Flesch, G. D.; Svec, H. J.; Gray, A. L.; Taylor, C. E. *Anal. Chem.* **1980**, *52*, 2283-2289.

(2) Houk, R. S.; Fassel, V. A.; Svec, H. J., *Dynamic Mass Spectrom.* **1981**, *6*, 234-251.

(3) Tan, S. H.; Horlick, G. *Applied Spectrosc.* **1986**, *40*, 445-460.

(4) Vaughan, M. A.; Horlick G. *Applied Spectrosc.* **1986**, *40*, 434-445.

(5) Lam, J. W.; McLaren, J. W. *J. Anal. At. Spectrom.* **1990**, *5*, 419-424.

(6) McLaren, J. W.; Lam, J. W.; Gustavsson, A. *Spectrochim. Acta , Part B* **1990**, *45B*, 1091-1094.

(7) Lam, J. W.; Horlick, G. *Spectrochim. Acta , Part B* **1990**, *45B*, 1313-1325.

(8) Jarvis, K. E.; Gray, A. L.; McCurdy, E. *J. Anal. At. Spectrom.* **1989**, *4*, 743-747.

(9) Vaughan, M.-A.; Templeton, D. M. *Applied Spectrosc.* **1990**, *44*, 1685-1689.

(10) Boorn, A. W; Browner, R. F. *Anal. Chem.* **1982**, *54*, 1402-1410.

(11) Hausler, D. W; Taylor, L. T. *Anal. Chem.* **1981**, *53*, 1223-1227.

(12) Hausler, D. W; Taylor, L. T. *Anal. Chem.* **1981**, *53*, 1227-1231.

(13) Kreuning, G.; Maessen, F. J. M. J. *Spectrochim. Acta , Part B* **1989**, *44B*, 367-384.

(14) Maessen, F. J. M. J.; Kreuning, G.; Balke, J. *Spectrochim. Acta , Part B* **1986**, *41B*, 3-25.

(15) Maessen, F. J. M. J.; Seeverens, P. J. H.; Kreuning, G. *Spectrochim. Acta, Part B* **1984**, *39B*, 1171-1180.

(16) Brotherton, T.; Barnes, B.; Vela, N.; Caruso, J. A. *J. Anal. At. Spectrom.* **1987**, *2*, 389-396.

(17) Brotherton, T. J.; Pfannerstill, P. E.; Creed, J. T.; Heitkemper, D. T.; Caruso, J. A.; Prastsinis, S. E. *J. Anal. At. Spectrom.* **1989**, *4*, 341-345.

(18) Magyar, B.; Lienemann, P.; Vonmont, H. *Spectrochim. Acta, Part B* **1986**, *41B*, 27-38.

(19) Ebdon, L.; Evans, E. H.; Barnett, N. W. *J. Anal. At. Spectrom.* **1989**, *4*, 505-508.

(20) Tsukahara, R.; Kubota, M. *Spectrochim. Acta, Part B* **1990**, *45B*, 581-589.

(21) Gustavsson, A. *Spectrochim. Acta, Part B* **1987**, *42B*, 111-118.

(22) Bäckström, K.; Gustavsson, A.; Hietala, P. *Spectrochim. Acta, Part B* **1989**, *44B*, 1041-1048.

(23) Gustavsson, A. *Spectrochim. Acta, Part B* **1988**, *43B*, 917-922.

(24) Gustavsson, A. *Trends Anal. Chem.* **1989**, *8*, 336-338.

(25) Gustavsson, A.; Hietala, P. *Spectrochim. Acta, Part B* **1990**, *45B*, 1103-1108.

(26) Park, C. J.; Van Loon, J. C.; Arrowsmith, P.; French, J. B. *Canad. J. Spectrosc.* **1987**, *32*, 29-36.

(27) Jiang, S. J.; Houk, R. S. *Spectrochim. Acta, Part B* **1987**, *42B*, 93-100.

(28) Gray, A. L. *Analyst* **1985**, *110*, 551-556.

(29) Wiederin, D. R.; Houk, R. S.; Winge, R. K.; D'Silva, A. P. *Anal. Chem.* **1990**, *62*, 1155-1160.

(30) Scott, R. H.; Fassel, V. A.; Kniseley, R. N.; Nixon, D. E. *Anal. Chem.* **1974**, *46*, 75-80.

(31) Shibata, N.; Fudagawa, N.; Kubota, M. *Anal. Chem.* **1991**, *63*, 636-640.

(32) McLeod, C. W.; Date, A. R.; Cheung, Y. Y. *Spectrochim. Acta, Part B* **1986**, *41B*, 169-174.

(33) Date, A. R.; Cheung, Y. Y.; Stuart, M. E. *Spectrochim. Acta, Part B* **1987**, *42B*, 3-20.

(34) Armentrout, P. B.; Beauchamp, J. L. *Chemical Physics* **1980**, *50*, 21-25.

(35) Weast, R. C. *Handbook of Chemistry and Physics*, 67th ed.; CRC: Boca Raton, FL, 1987.

PAPER II.

MEASUREMENT OF VANADIUM, NICKEL, AND ARSENIC IN SEAWATER AND URINE REFERENCE MATERIALS BY INDUCTIVELY COUPLED PLASMA MASS SPECTROMETRY WITH CRYOGENIC DESOLVATION

ABSTRACT

Addition of a small dose (2%) of H_2 to the aerosol gas flow enhanced analyte signals by a factor of 2 to 3, which compensated for the loss of analyte signal that accompanied earlier efforts at cryogenic desolvation with inductively coupled plasma mass spectrometry (ICP-MS). Vanadium, nickel, and arsenic at μg L^{-1} levels in urine, river, and seawater reference materials were determined. The polyatomic ions ClO^+, CaO^+, and $ArCl^+$, which normally cause severe overlap interferences for these elements, were attenuated to manageable levels by cryogenic desolvation. The samples were simply diluted with 1% HNO_3 so that the chloride could be removed as HCl. The analytical results obtained for these standard reference materials agreed closely with the certified or recommended values. The detection limit ranges (3σ) obtained were 10–1000 ng L^{-1} for V, 0.03–20 μg L^{-1} for Ni, and 4–7000 ng L^{-1} for As in the original samples. The samples were introduced by flow injection to minimize clogging of the sampling orifice.

INTRODUCTION

ICP-MS is a powerful technique for the measurement of trace elements but is not always readily applicable for all elements in every conceivable sample. The determination of V, Ni, and As by ICP-MS is very troublesome (1–4) if the sample matrix contains large amounts of chlorine and calcium; $ArCl^+$ overlaps As^+, $^{35}Cl^{16}O^+$ overlaps $^{51}V^+$, and CaO^+ and $CaOH^+$ overlap various Ni^+ isotopes. Generally, Cl and Ca are either removed by chemical separation procedures (2–8), or correction procedures such as principal component analysis (1) or multivariate calibration (9) are used. The atomic analyte ions can also be separated from the interfering polyatomic ions with a high resolution mass spectrometer (10,11).

A recent paper (12) showed that cryogenic desolvation can attenuate troublesome MO^+ ions to very low levels (0.02 – 0.05%), presumably by removing the nebulized water and reducing the corresponding density of oxygen in the ICP. Chloride can also be removed as HCl in the same way (12). The present paper critically examines the actual performance of cryogenic desolvation for the measurement of several difficult elements (V, Ni, and As) in troublesome matrices such as urine and seawater.

This work also uses an Ar-H_2 mixed gas plasma to improve the sensitivity obtained with cryogenic desolvation. Several varieties of mixed-gas plasmas have been described for ICP-MS including plasmas with N_2 in the outer gas (13–16) and N_2, O_2, CH_4, He, or Xe mixed with Ar in the aerosol gas (17–20). Shibata *et al.* add a small dose of H_2 to the aerosol gas flow, which improves analyte signals when electrothermal vaporization is used for sample introduction (21). Addition of H_2 would be expected to have similar beneficial effects for the dry plasma produced

during cryogenic desolvation. Murillo and Mermet also report that adding a few percent of H_2 as a swirling sheath around the aerosol gas flow improves ionization and excitation in ICP atomic emission spectrometry (22). Finally, the sample was introduced by flow injection to minimize deposition of solids on the sampling orifice (23–26). The sampler would clog in a few minutes if the difficult urine and seawater matrices were introduced continually with the ultrasonic nebulizer used in the present work.

EXPERIMENTAL SECTION

Sample Preparation and Standard Solutions

Three water reference samples were analyzed: a riverine water (SLRS-2), an estuarine water (SLEW-1, ~ 1% total salts), and a nearshore seawater (CASS-2, ~ 3% total salts) (Marine Analytical Chemistry Standards Program, Division of Chemistry, National Research Council of Canada (NRCC), Ottawa, Ontario, Canada K1A OR6). SLEW-1 was diluted tenfold with 1% HNO_3, CASS-2 was diluted 30-fold, and SLRS-2 was used neat. In addition, two freeze-dried urine reference samples were obtained from NIST (SRM 2670 - normal and elevated levels). The urine samples were reconstituted and diluted 100-fold in deionized distilled water. With the exception of SLRS-2, all samples were diluted to avoid blockage of the sampler and skimmer cones and to reduce the extent of signal suppression due to the matrix. Both water and urine samples were acidified with HNO_3 to 1%. No chemical separations or other sample pretreatment procedures were necessary.

Distilled deionized water was obtained from a Barnstead Nanopure-II system (18 MW, Barnstead Co., Newton, MA). Standard solutions were prepared from 1000 mg L^{-1} standards from Fisher Scientific (Fair Lawn, NJ) with a 1% nitric acid solution (Ultrex II Ultrapure reagent grade, J. T. Baker, Phillipsburgh, NJ).

The method of standard additions was employed. The solutions of SLEW-1 and CASS-2 were spiked with 0, 10, 15, 20, and 25 ng L^{-1} of V, Ni, and As. The solutions of SLRS-2 contained an additional 0, 1, 2, 4, and 6 µg L^{-1} of V, Ni, and As. Both urine samples (normal and elevated levels) were spiked with an additional 0, 1, 2, 3, and 4 µg L^{-1} of V, Ni, and As. Blank solutions were prepared that contained only the major sample constituents at the concentrations cited on certificates.

V, Ni, and As were determined concomitantly and in triplicate. Least square lines were fit to the data and plots were generated of the analyte count rate versus spike concentration. The ratio between the intercept and slope values gave the concentration of the analyte in the sample. Typically the correlation coefficient of the least squares fit ranged from 0.97 to 0.9999.

Instrumentation

Typical operating conditions are listed in Table 1. A Perkin-Elmer Sciex ELAN Model 250 ICP mass spectrometer with upgraded ion optics and software was used. The sample nebulization and desolvation schemes used were described in a previous paper (12). The argon aerosol gas flow rate was adjusted daily to maximize signal for La^+. This optimization generally required a rather high aerosol gas flow rate of ~ 1.9 L min^{-1}. The voltages applied to the ion lenses generally did not require adjustment from day to day. Hydrogen was added to the aerosol flow through the side arm of a small tee (5 mm i.d.) at the base of the torch. The argon carrying the aerosol passed straight through the tee into the injector tube of the torch. The H_2 flow was ~ 2% of the total aerosol flow rate except where stated otherwise. Both the H_2 and Ar flows were regulated by a mass flow controller. Samples were injected with a Rheodyne, low pressure, six port, metal free flow injection valve with a 500 µL Teflon sample loop (Altech Associates, Deerfield, IL).

Data Acquisition

Data were acquired in the multielement mode at low resolution setting (1 amu width at 10% valley) with three measurements per peak, 250-ms dwell time,

Table 1. Operating conditions

ICP torch	Ames Laboratory design (27); outer tube extended 30 mm from inner tubes
Plasma forward power	1.25 kW
Gas flow rates (L min^{-1})	
Outer Ar	12
Auxiliary Ar	0.4
Aerosol	
Ar	1.9
H_2	0.0388 (2% of total aerosol flow)
Sampling position	20 mm above load coil, on center
Sampler	Copper, 1.1 mm diam. orifice
Skimmer	Nickel, 0.9 mm diam. orifice
Ion lens settings	
Bessel box stop	- 5.9 V
Bessel box barrel	+ 5.4 V
Bessel box plate	- 11.0 V
Einzel 1 and 3	- 19.8 V
Einzel 2	- 130.0 V
Electron multiplier voltage	- 4000 V
Ultrasonic Nebulizer	Cetac Technologies (Omaha, NE) Model U-5000 current setting = 6 (arbitrary units) desolvation heater temp. = 140°C desolvation condenser temp. = 0°C
Cryocooler	Cryocool CC-100II at - 80°C Neslab (Portsmouth, NH)

and 0.75-s measurement time. Count rates were not corrected for isotopic overlap, i.e., between different analyte elements such as $^{58}Ni^{+}$ and $^{58}Fe^{+}$. The count rates recorded for each flow-injection peak were first smoothed with a three-point moving average. The height of each peak was then measured and corrected for background for the appropriate matrix blank solution. Detection limits were calculated as the analyte concentrations necessary to yield net signals equivalent to three times the standard deviation of 20 measurements of the background.

RESULTS AND DISCUSSION

Effect of H_2 on M^+ Sensitivity and MO^+/M^+ Ratio

In previous work, cryogenic desolvation reduced the M^+ signal by about 50%, compared to that obtainable by desolvation with a single condenser at 0°C (12). The copper cryogenic loops may have trapped some of the analyte. An experiment was performed to verify how much analyte was actually lost in the loops. A 100 mg L^{-1} Ho solution was nebulized for 2.5 hours. The ice trapped in the cryocooler loops was melted and analyzed for its Ho content. The water deposited in the drain of the spray chamber and in the first condenser (at ~ 0°C) was also collected. The amount of Ho found in the cryogenic loops corresponded to only 0.1% of the net amount of Ho that left the ultrasonic nebulizer. Therefore, the cryogenic loops were not responsible for the large loss of Ho. The decrease in analyte signal must be due to the drastic decrease in the water loading in the plasma when cryogenic desolvation is used.

Fortunately, a judicious choice of mixed gas plasma can boost analyte signals in this case. Adding 3% H_2 to the aerosol gas flow increased the La^+ signal four-fold during cryogenic desolvation (Figure 1A). Similar enhancements were seen for other analyte elements. In contrast, adding H_2 suppressed La^+ signal when cryogenic desolvation was not used. The addition of 3% H_2 boosted the La^+ signal during cryogenic desolvation well above that obtained when conventional desolvation was used, for reasons that are unclear.

The effect of H_2 dose on oxide ratios for LaO^+/La^+ is shown in Figure 2. During cryogenic desolvation (Figure 2A) the addition of H_2 induced a welcome decrease in LaO^+/La^+ from 0.06% (at 0% H_2) to 0.02% at 2–3% H_2. The reader

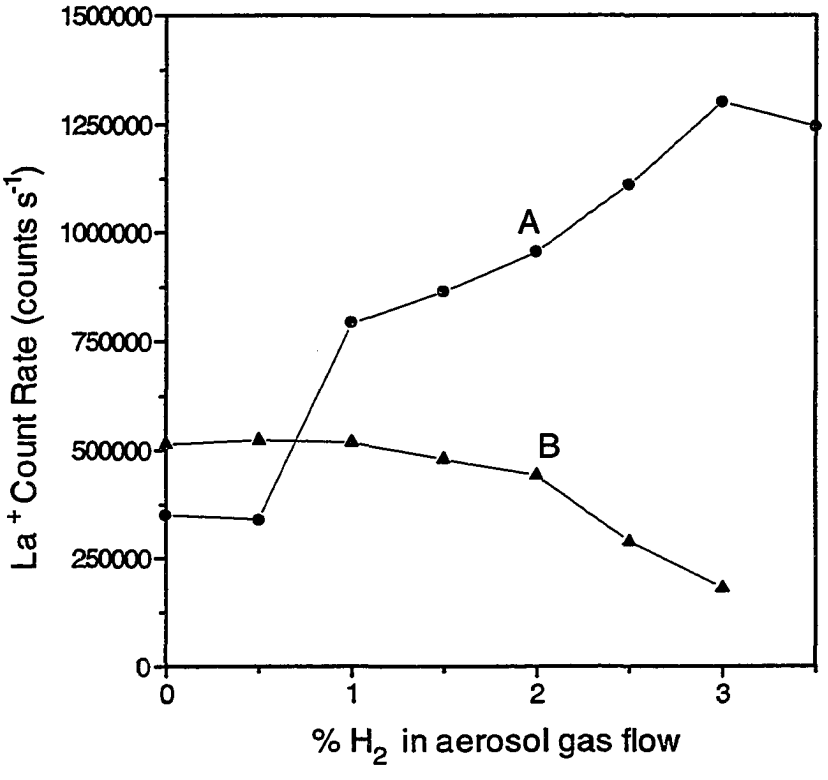

Figure 1. Effect of H_2 dose in aerosol gas flow on La^+ signal (a) with cryogenic desolvation and (b) without cryogenic desolvation. The La concentration was 100 μg L^{-1}.

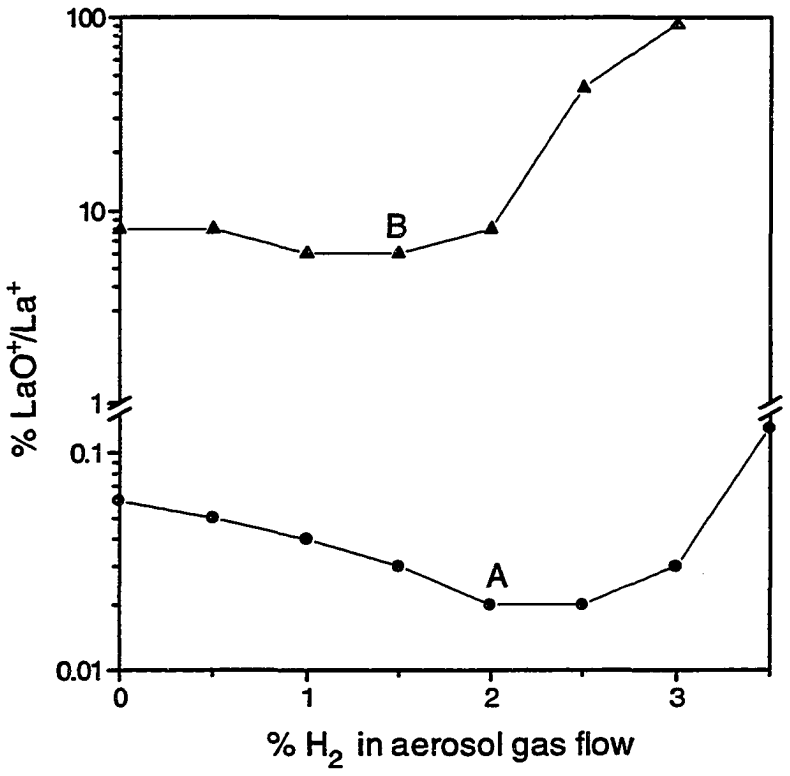

Figure 2. Effect of H_2 dose in aerosol gas flow on abundance of LaO^+ relative to La^+ (a) with cryogenic desolvation and (b) without cryogenic desolvation. The La concentration was 100 $\mu g\ L^{-1}$.

should note that these oxide ratios were obtained at the aerosol gas flow rate that maximized La^+ signal (28). Hydrogen doses above 3% caused the LaO^+/La^+ ratio to increase, and the plasma also became unstable at higher H_2 doses. Therefore, the H_2 level was kept at 2% in the aerosol gas flow for the work reported below. Without cryogenic desolvation (Figure 2B) the oxide ratios were much higher (≥ 7%), and they actually deteriorated as more H_2 is added. Thus adding extra H_2 was beneficial only when the solvent load was very low.

Sample Analyses

The samples analyzed in this study contained different amounts of chlorine, largely as NaCl and KCl. In the previous paper (12), cryogenic desolvation reduced dramatically the amounts of Cl^+, ClO^+, and $ArCl^+$ observed when a 1% HCl solution was nebulized. HCl has a low boiling point (-84.9°C) and high melting point (-114.8°C) (29) and therefore it is easily trapped in the cryogenic loops. However, a salt such as NaCl, which has a very high boiling point (1413°C) (29), would not be removed by cryogenic desolvation. Fortunately, much of the chloride from these salt solutions can be removed as HCl by simply adding an excess of HNO_3, so that the volatile HCl is formed when the aerosol droplets are desolvated. The Na^+ and K^+ remain behind, presumably as $NaNO_3$ and KNO_3, hence standard additions are used to compensate for the resulting matrix interference.

For those analytes and samples that were measured, the count rates from the matrix blanks are listed in Table 2. The matrix blanks contain the troublesome interfering element (i.e., Cl^- for V and As, Ca^{2+} for Ni) at the same concentration listed on the certificate for each reference material. After each blank was measured, the unspiked sample of interest was analyzed next; the net count rate observed from

Table 2. Net count rates and typical count rates for matrix blanks.

	V (m/z = 51)		As (m/z = 75)		Ni (m/z = 58)		Ni (m/z = 60)	
Sample	from sample (counts s^{-1}, net)	from blank (counts s^{-1})	from sample (counts s^{-1}, net)	from blank (counts s^{-1})	from sample (counts s^{-1}, net)	from blank (counts s^{-1})	from sample (counts s^{-1}, net)	from blank (counts s^{-1})
Urine (normal) NIST SRM 2670	420	190±30	930	190±65	1570	3360±195	840	710±60
Urine (elevated) NIST SRM 2670	4700	95±20	5400	40±10	6000	370±40	2450	130±5
Riverine water NRCC SLRS-2	580	65±10	365	25±5	680	250±15	270	105±10
Estuarine water NRCC SLEW-1	650	450±60	87	170±5	-	-	-	-
Nearshore seawater NRCC CASS-2	100	110±15	16	100±2	-	-	-	-

each unspiked sample is also listed in Table 2. Finally, Tables 3, 4, and 5 present the concentration measurements and detection limits. These results are now discussed individually for each element. Nickel was not measured in the seawater samples, for no particular reason.

Vanadium Measurements

Vanadium has two isotopes: ^{50}V (0.25%) and ^{51}V (99.75%); the only abundant one suffers overlap from $^{35}Cl^{16}O^+$. Analytical results are presented in Table 3 for the V concentrations in the reconstituted freeze-dried urine and water samples. The determined and accepted concentrations for V agree well in the river water SLRS-2, which is an easy sample because it does not contain much chlorine. The measured V concentration for NIST urine is 100±10 $\mu g\ L^{-1}$, which seems a little low, although this result could still be within the interval around the information value of 120 $\mu g\ L^{-1}$ provided by NIST. Neither NIST nor NRCC provides vanadium concentrations for the normal urine and seawater samples, largely because of the ClO^+ interference on $^{51}V^+$. The detection limits obtained for V were 1000, 1000, 10, 150, and 500 ng L^{-1} for urine (normal), urine (elevated), SLRS-2, SLEW-1, and CASS-2, respectively.

Although the blank count rates at m/z = 51 (Table 2) are much lower than usual from highly saline samples, the blank count rates are still significant relative to the sample count rates. Subtraction of the blank at m/z = 51 is still necessary. For example, the V concentration for CASS-2 would have been too high by a factor of two without such a correction. Sensitivities for $^{51}V^+$ in these samples were $2x10^6$ to $8x10^6$ counts s^{-1} per mg L^{-1} V and varied within this range on different days, as was the case for the other sensitivity values cited below.

Table 3. Vanadium Measurements

Sample	Approximate Cl^- conc. (mg L^{-1})	V conc. (μg L^{-1})[a] Measured[b]	Certified or (information) value	Estimated detection limits (ng L^{-1})[d]
Urine (normal) NIST SRM 2670	4400	20±4	-	1000
Urine (elevated) NIST SRM 2670	4400	100±10	(120)	1000
River water NRCC SLRS-2	< 10	0.24±0.03	0.25±0.06	10
Estuarine water NRCC SLEW-1	10,000	0.79±0.0012	-	150
Nearshore seawater NRCC CASS-2	30,000	2.60±0.0089	-	500

[a] Vanadium concentrations are corrected to those in the original samples.

[b] Uncertainties are standard deviations of triplicate analyses.

[c] Standard deviation given is 1σ.

[d] Values cited are for the original sample, i.e., they are corrected for dilution.

Table 4. Arsenic Measurements

Sample	Approximate Cl^- conc. (mg L^{-1})	As conc. (μg L^{-1})[a] Measured[b]	Certified or (information) value	Estimated detection limits (ng L^{-1})[d]
Urine (normal) NIST SRM 2670	4400	60±2	(60)	7000
Urine (elevated) NIST SRM 2670	4400	510±10	480±100	3000
River water NRCC SLRS-2	< 10	0.78±0.01	0.77±0.09	4
Estuarine water NRCC SLEW-1	10,000	0.74±0.01	0.765±0.093	30
Nearshore seawater NRCC CASS-2	30,000	1.05±0.01	1.01±0.07	90

[a] Arsenic concentrations are corrected to those in the original samples.

[b] Uncertainties are standard deviations of triplicate analyses.

[c] Standard deviation given is 1σ.

[d] Values cited are for the original sample, i.e., they are corrected for dilution.

Table 5. Nickel Measurements

Sample	Ca conc. (mg L^{-1})	Ni conc. (μg L^{-1})[a] Measured ($^{58}Ni^{+}$)[c]	Measured ($^{60}Ni^{+}$)[c]	Certified or (information) value	Estimated detection limits (μg L^{-1})[d]
Urine (normal) NIST SRM 2670	105	76±4	70±1	(70)	20
Urine (elevated) NIST SRM 2670	105	300±20	300±1	(300)	10
River water NRCC SLRS-2	5.70	1.04±0.01	1.01±0.02	1.03±0.10	0.03

[a] Nickel concentrations are corrected to those in the original samples.

[b] Standard deviation given is 1σ.

[c] Uncertainties are standard deviations of triplicate analyses.

[d] Values for ^{58}Ni; values cited are for the original sample, i.e., they are corrected for dilution.

Arsenic Measurements

Arsenic is monoisotopic at m/z = 75 and is prone to interference from $^{40}Ar^{35}Cl^{+}$. The results of the analyses are given in Table 4 for the As concentrations in the urine and water samples. The determined and accepted concentrations for As agree closely for all the samples tested. The detection limits obtained for As were 7000, 3000, 4, 30, and 90 ng L^{-1} for urine (normal), urine (elevated), SLRS-2, SLEW-1, and CASS-2 respectively.

The blanks for As in normal urine and seawater (Table 2) were significant. Remarkably, although the net count rate for As in CASS-2 is only 16 counts s^{-1}, and the blank is high (100 counts s^{-1}), the measured concentration (1.05 µg L^{-1}) in Table 4 is both accurate and precise. Sensitivity for As was $2x10^5$ to $2x10^6$ counts s^{-1} per mg L^{-1}.

Nickel Measurements

The two major nickel isotopes (^{58}Ni and ^{60}Ni) are subject to interferences from CaO^{+}, the major problems being $^{42}Ca^{16}O^{+}$, $^{40}Ca^{18}O^{+}$, and $^{44}Ca^{16}O^{+}$. The same cryogenic conditions that remove HCl also greatly reduce the water loading, which is probably the major source of the oxygen in CaO^{+} (12). As shown in Table 5, Ni could be measured accurately in urine and river water. The detection limits obtained for Ni (using m/z = 58) were 20, 10, and 0.03 µg L^{-1} for urine (normal), urine (elevated), and SLRS-2 respectively.

The blank count rates for m/z = 58 to those at m/z = 60 are ~ 2/1, which shows that each blank was likely contaminated somewhat with Ni. Alternatively, some Ni^{+} could have been produced from the skimmer, which was constructed from Ni.

These blank count rates are not primarily from $^{42}Ca^{16}O^+$ and $^{44}Ca^{16}O^+$, as ^{42}Ca is three times less abundant than ^{44}Ca. Nevertheless, the measured concentrations for Ni (Table 5) are reasonably accurate and precise. For $^{58}Ni^+$, corrections for $^{58}Fe^+$ were derived by measuring $^{57}Fe^+$; these corrections were negligible. The sensitivity for $^{58}Ni^+$ was $7x10^5$ to $2x10^6$ counts s^{-1} per mg L^{-1}.

In general the sensitivities listed above for all three elements are similar to those in our previous paper on cryogenic desolvation (12). Apparently, the enhancement of sensitivity produced by H_2 balanced the expected matrix effects from seawater and urine. The detection limits are now somewhat worse than would be expected from previous paper (12) when the various dilution factors (10, 30 or 100) are considered, mainly because of the significant blanks observed.

CONCLUSION

The value of cryogenic desolvation with ICP-MS for the quantification of V, Ni, and As in matrices containing Ca and Cl^- has been demonstrated convincingly. The addition of hydrogen to the central channel improved the analyte sensitivity but kept oxide ratios low. The basic reasons for these beneficial effects of H_2 in a dry ICP are intriguing and are the subject of further study.

ACKNOWLEDGMENTS

The loan of an ultrasonic nebulizer from Cetac Technologies, Inc., is gratefully acknowledged.

CREDIT

Ames Laboratory is operated by Iowa State University for the U. S. Department of Energy under Contract No. W-7405-Eng-82. This research was supported by the Office of Basic Energy Sciences, Division of Chemical Sciences.

SAFETY NOTE

Care should be observed when handling hydrogen. A back-flow-prevention valve was installed on the cylinder and the hydrogen flow was severed before the plasma was turned off. Caution should also be observed when handling V, Ni, and As because of their toxicity and carcinogenic properties.

LITERATURE CITED

(1) Vaughan, M. -A.; Templeton, D. M. *Appl. Spectrosc.* **1990**, *44*, 1685-1689.

(2) Plantz, M. R.; Fritz, J. S.; Smith, F. G.; Houk, R. S. *Anal. Chem.* **1989**, *61*, 149-153.

(3) Beauchemin, D.; Berman, S. S. *Anal. Chem.* **1989**, *61*, 1857-1862.

(4) McLaren, J. W.; Mykytiuk, A. P.; Willie, S. N.; Berman, S. S. *Anal. Chem.* **1985**, *57*, 2907-2911.

(5) Lyon, T. D. B.; Fell, G. S.; Hutton, R. C.; Eaton, A. N. *J. Anal. At. Spectrom.*, **1988**, *3*, 601.

(6) Sheppard, B. S.; Shen, W. L.; Caruso, J. A.; Heitkemper, D. T.; Fricke, F. L. *J. Anal. Atom. Spectrom.* **1990**, *5*, 431-435.

(7) Lyon, T. D. B.; Fell, G. S.; Hutton, R. C.; Eaton, A. N. *J. Anal. At. Spectrom.*, **1988**, *3*, 265.

(8) Branch, S.; Corns, W. T.; Ebdon, L.; Hill, S.; O'Neill, P. *J. Anal. At. Spectrom.*, **1991**, *6*, 155.

(9) Ketterer, M. E.; Biddle, D. A. *Anal. Chem.* **1992**, *64*, 1819-1823.

(10) Bradshaw, N.; Hall, E. F. H.; Sanderson, N. E. *J. Anal. At. Spectrom.* **1989**, *4*, 801-803.

(11) Morita, M.; Ito, H.; Uehiro, T.; Otusuka, K. *Anal. Sci (Japan)* **1989**, *5*, 609-610.

(12) Alves, L. C.; Wiederin, D. R.; Houk, R. S. *Anal. Chem.* **1992**, *64*, 1164-1169.

(13) Houk, R. S.; Montaser, A.; Fassel, V. A. *Appl. Spectrosc.* **1983**, *37*, 425-428.

(14) Beauchemin, D.; Craig, J. M. *Spectrochim. Acta, Part B* **1991**, *46B*, 603-614.

(15) Lam, J. W. H.; Horlick, G. *Spectrochim. Acta, Part B* **1990**, *45B*, 1313-1325.

(16) Lam, J. W. H.; McLaren, J. W. *J. Anal. Atomic Spectrom.* **1990**, *5*, 419-424.

(17) Evans, E. H.; Ebdon, L. *J. Anal. Atomic Spectrom.* **1984**, *4*, 299-300; **1990**, *5*, 425-430.

(18) Sheppard, B. S.; Shen, W. -L.; Davidson, T. M.; Caruso, J. A. *J. Anal. Atomic Spectrom.* **1990**, *5*, 697-700.

(19) Sheppard, B. S.; Shen, W. -L.; Caruso, J. A. *J. Amer. Soc. Mass Spectrom.* **1991**, *2*, 355-361.

(20) Smith, F. G.; Wiederin, D. R.; Houk, R. S. *Anal. Chem.* **1991**, *63*, 1458-1462.

(21) Shibata, N.; Fudagawa, N.; Kubota, M. *Anal. Chem.* **1991**, *63*, 636-640.

(22) Murillo, M.; Mermet, J. M. *Spectrochim. Acta, Part B* **1989**, *44B*, 359-366.

(23) Houk, R. S.; Thompson, J. J. *Biomed. Mass Spectrom.* **1983**, *10*, 107-112.

(24) Vickers, G. H.; Ross, B. S.; Hieftje, G. M. *Appl. Spectrosc.* **1989**, *43*, 1330-1333.

(25) Jarvis, K. E.; Gray, A. L.; Houk, R. S. *Handbook of ICP-MS*, Blackie: London, **1992**, p. 119.

(26) Beauchemin, D. *Trends Anal. Chem.* **1991**, *10*, 71-77.

(27) Scott, R. H.; Fassel, V. A.; Kniseley, R. N.; Nixon, D. E. *Anal. Chem.* **1974**, *46*, 75-80.

(28) Vaughan, M. A.; Horlick, G. *Appl. Spectrosc.* **1986**, *40*, 434-445.

(29) Weast, R. C. *Handbook of Chemistry and Physics*, 67th ed.; CRC: Boca Raton, FL, **1987**.

PAPER III.

REMOVAL OF ORGANIC SOLVENTS BY CRYOGENIC DESOLVATION IN INDUCTIVELY COUPLE PLASMA MASS SPECTROMETRY

ABSTRACT

Methanol, ethanol, acetone, or acetonitrile were nebulized continuously with an ultrasonic nebulizer. The solvent was then removed from the aerosol stream by repetitive heating at ~ 100°C and cooling in a set of cryogenic loops at -80°C. Ethanol was the only solvent that required additional O_2 (1-5%) in the aerosol gas to prevent carbon deposition on the sampler. Oxide ratios for LaO^+/La^+ and UO^+/U^+ were 0.03% to 0.1%. Cryogenic desolvation attenuated but did not eliminate the usual carbon-containing polyatomic ions (e.g., CO^+, CO_2^+, ArC^+, and $ArCO^+$). Analyte sensitivities from metal nitrate salts in methanol were comparable to each other and to the sensitivities from aqueous metal solutions. Substantial memory effects were observed from several metal complexes.

INTRODUCTION

The introduction of organic solvents into an ICP is beset with problems (1–8). Generally, volatile organic solvents overload the plasma, so that a high forward power is necessary to stabilize the discharge (9). In ICP-MS, carbon deposits on the interface, numerous polyatomic ions such as CO^+, ArC^+, $ArCO^+$, and MC^+ (M = metal) are observed, and the sensitivity and detection limits for analyte ions are usually poorer than those obtained when aqueous solutions are nebulized (10, 11).

These problems are severe enough that many analysts prefer to simply digest organic samples and introduce them as aqueous solutions. When organic solvents can not be avoided, most analysts use only relatively nonvolatile ones such as xylene or methyl isobutyl ketone. A small dose of O_2 is often added to the aerosol gas to prevent carbon deposition (10–12). As might be expected, this remedy tends to increase spectral overlap problems from metal oxide ions (MO^+).

Removal of the solvent after nebulization is one general solution to these problems. Maessen and co-workers have examined this remedy thoroughly for ICP emission spectrometry (5). Cryogenic desolvation at -77°C was used by Wiederin *et al.* for the analysis of organic solvents by ICP atomic emission spectrometry. Essentially, the plasma operated stably at forward power levels of only ~ 1 kW when cryogenic desolvation was employed. Analyte emission sensitivity was similar to that obtained from aqueous solutions, and interferences from molecular bands were minimal (13).

Cryogenic desolvation has proven very valuable for removal of water and HCl from aqueous samples in ICP-MS (14, 15). The current paper extends this work to organic solvents. Hill and co-workers have recently described a condensation system based on Peltier coolers for analysis of organic solvents by ICP-MS. They could not cool the aerosol below -40°C, and they noted the probable advantage of removing more solvent by cooling the aerosol at still lower temperatures (12). The solvents studied in the present work are relatively volatile and are usually considered among the more "difficult" ones for introduction into the ICP (16). The performance of cryogenic desolation for simple inorganic salts is also compared to that for relatively volatile metal complexes.

EXPERIMENTAL SECTION

Instrumentation and Data Acquisition

A Perkin-Elmer Sciex ELAN Model 250 ICP mass spectrometer with upgraded ion optics and software was used. Typical operating conditions are listed in Table 1. Note that an ultrasonic nebulizer (18, 19) was used. Operating conditions were optimized daily to maximize signal for La^+. The liquid flow rate was 1.5 mL min^{-1}.

The cryogenic desolvation system is shown in Figure 1. This apparatus follows the standard condenser provided with the nebulizer. The bulk of the organic solvent condensed in the first glass loops. This condensed solvent was still liquid, which was drained off periodically through Tygon tubing under the loops. The aerosol was then heated and cooled repeatedly in a set of copper loops like those used for aqueous solvents (14). This process dried the aerosol thoroughly. Without the heating steps, solvent tended to condense back from the vapor phase onto the sample particles in the cold loops. These wet droplets were then transported readily to the plasma, as noted previously by Maessen *et al.* (5) and Wiederin *et al.* (13).

Peak hopping data were acquired in the multielement mode at low resolution setting (1 amu width at 10% valley) with 3 measurements per peak, 20 ms dwell time, and 1 s measurement time. Spectra were acquired in the sequential mode with 10 measurements per peak and a 1 s measurement time. Count rates were not corrected for isotopic overlaps.

Table 1. Typical operating conditions

ICP torch	Ames Laboratory design (17); outer tube extended 30 mm from inner tubes
Plasma forward power	1.25 – 1.5 kW
Argon flow rates (L min^{-1})	
Outer	12
Auxiliary	0.3
Aerosol	1.6
Sampling position	20 mm above load coil, on center
Sampler	Copper, 1.1 mm diam. orifice
Skimmer	Nickel, 0.9 mm diam. orifice
Ion lens settings	
Bessel box stop	- 5.9 V
Bessel box barrel	+ 5.4 V
Bessel box plate	- 11.0 V
Einzel 1 and 3	- 19.8 V
Einzel 2	- 130.0 V
Electron multiplier voltage	- 4000 V
Ultrasonic Nebulizer	Cetac Technologies (Omaha, NE) Model U-5000 current setting = 6 (arbitrary units) desolvation heater temp. = dependent on solvent desolvation condenser temp. = -10°C
Cryocooler	Cryocool CC-100II at - 80°C Neslab (Portsmouth, NH)

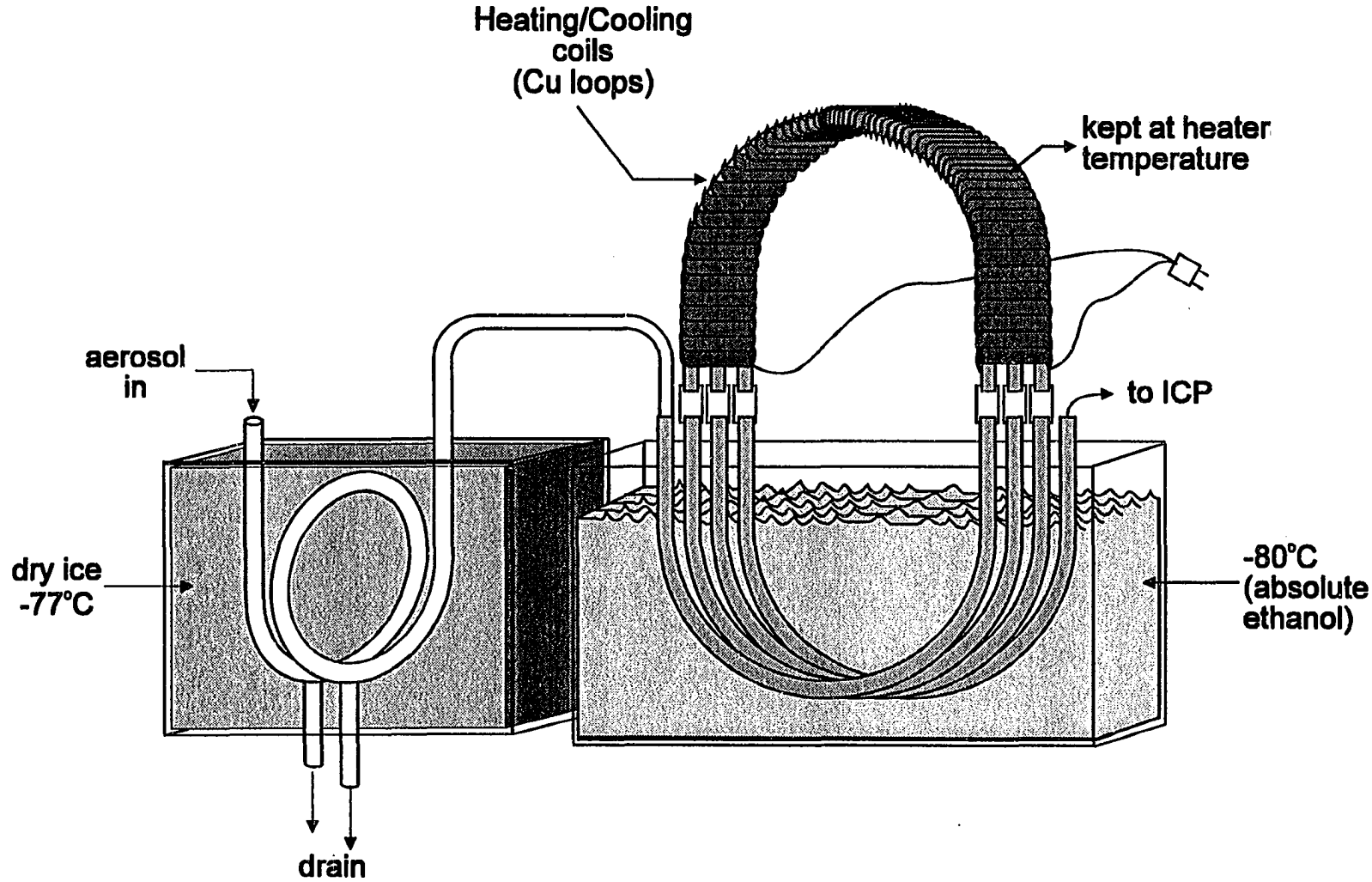

Figure 1. Diagram of cryogenic desolvation device for organic solvents.

Chemicals and Standard Solutions

HPLC grade organic solvents were used for all experiments (Fisher Scientific Co.). Standard solutions were prepared by diluting aliquots from 1000 mg L^{-1} aqueous standards (PlasmaChem, Farmingdale, NJ) with methanol. The aqueous standards were supplied as nitrate salts.

For comparative purposes, stock solutions of metal complexes with various ligands were also prepared. These analyte compounds were selected to represent a range of melting and boiling points. Metal acetate stock solutions were prepared by dissolving analytical reagent grade acetate salts of Zn, Co, and Mn (Fisher Scientific Co.) at 1 mg L^{-1} in methanol. Cobalt tricarbonyl nitrosyl ($Co(CO)_3NO$), yttrium acetylacetonate ($Y(acac)_3$), and niobium ethoxide ($Nb(OC_2H_5)_5$) (Strem Chemicals, Inc., Newburyport, MA) were weighed and dissolved completely in methanol to give solutions that were 1 mg L^{-1} of the metal. Analyte solutions were then made by further dilution from these stock solutions.

RESULTS AND DISCUSSION

General Observations

The solvents and analyte compounds studied and their melting and boiling points are given in Table 2. As noted previously (13), the ultrasonic nebulizer produces an extremely intense aerosol from these solvents. Nevertheless, the plasma ignites easily and operates stably at moderate forward powers of 1.25 – 1.5 kW. After ignition, the axial channel is punched by simply turning on the aerosol gas flow during nebulization of the solvent. The heater temperature is selected to be 40°C above the boiling point of the solvent, as noted previously (13).

Methanol and acetonitrile can be nebulized indefinitely without noticeable green C_2 emission or deposition of carbon on the sampler. Substantial carbon deposition and C_2 emission are observed when ethanol is nebulized. In this case, oxygen is added to the aerosol flow through the side arm of a small tee (5 mm i.d.) at the base of the torch. The argon carrying the aerosol passes straight through the tee into the injector tube of the torch. The additional oxygen burns off the carbon deposited on the sampling cone. Oxygen is bled in gradually until the O_2 flow rate is just high enough to remove the green C_2 emission. This O_2 flow is typically 1-5% of the total gas flow into the center of the ICP.

When acetone is nebulized, a small amount of carbon deposits on the cone. Adding a brief burst of O_2 into the aerosol gas flow for ~ 30 s every 2 hours removes this deposit. Continuous addition of O_2 is not necessary for the analysis of acetone.

The different behavior seen for these four solvents can be explained as follows. The cold loops are at -80°C, some 34°C below the melting point of acetonitrile (Table 2). Thus, the vapor pressure of acetonitrile at the exit of the

Table 2. Physical data for solvents and solutes and heater temperatures used

Solvent	m.p. (°C)	b.p. (°C)	Heater Temp. (°C)
Methanol	-93.9	65	105
Ethanol	-117.3	78.5	119
Acetone	-95.35	56.2	96
Acetonitrile	-45.7	81.6	122

Solute[a]	m.p. (°C)	b.p. (°C)
$Mn(CH_3COO)_2.4H_2O$	> 300	-
$Co(CH_3COO)_2.4H_2O$	> 270	-
$Zn(CH_3COO)_2.2H_2O$	248	-
$Co(CO)_3NO$	-	50
$Y(CH_3COCHCOCH_3)_3$	139	-
$Nb(OC_2H_5)_5$	6	142

[a] These solutes were introduced as methanol solutions, so the heater temp. was 105°C in each case.

cryocondenser is very low. The other three solvents have higher vapor pressures because the loop temperature is above their melting points. Methanol and acetone have almost the same melting points (~ -95°C), but acetone causes more C_2 emission and carbon deposition because it has a 2/1 molar excess of C relative to O. Ethanol has a still lower melting point and a 2/1 ratio of C/O. Thus, the solvent load out of the condenser is greatest for ethanol, and the stoichiometry of ethanol also favors carbon deposition and C_2 emission.

Background Spectra

Generally, the mass spectra from an ICP containing organic solvents show the usual major ions (e.g., Ar^+, ArH^+, Ar_2^+, O^+, ...), as well as substantial levels of additional polyatomic ions from the constituents of the solvent (10, 11). The count rates observed for four of the more troublesome polyatomic ions from each solvent are shown in Table 3. As expected, the count rates for these background ions vary with the solvent used, since a fixed loop temperature yields different solvent loads. When ethanol is nebulized, the addition of O_2 enhances the signals from all four of these ions, even ArC^+, which contains no oxygen. All four of these polyatomic ions are still abundant enough to cause problems, although less so than in previous experiments with organic solvents in ICP-MS (10, 11). No Cu^+ from the loops is detected when organic solvents are nebulized.

Analyte Sensitivity

Solutions containing La and U at 500 $\mu g\, L^{-1}$ in different solvents were nebulized to determine if analyte sensitivities varied among solvents. Table 4

Table 3. Count rates for polyatomic ions observed for various organic solvents

Solvent	Count rates (counts s^{-1})			
	CO^+ ($m/z = 28$)	CO_2^+ ($m/z = 44$)	ArC^+ ($m/z = 52$)	ArO^+ ($m/z = 56$)
Methanol	1.7×10^6	11,000	5,400	2500
Acetone	3.0×10^6	48,000	24,000	3000
Ethanol	1.5×10^6	29,000	15,000	1700
Ethanol + O_2	3.7×10^6	65,000	83,000	6400
Acetonitrile	1.2×10^5	24,000	15,000	6600

Table 4. Signals for La^+, U^+, and metal oxides (MO^+) in different solvents[a]

Species	methanol	acetonitrile	acetone	ethanol	ethanol+O_2[b]
La^+	$1.8x10^6$	$1.9x10^6$	$2.6x10^6$	$3.8x10^5$	$2.1x10^6$
U^+	$6.1x10^5$	$8.1x10^5$	$1.4x10^6$	$3.2x10^5$	$9.6x10^5$
LaO^+	766	655	1349	203	1759
LaO^+/La^+ (%)	0.04	0.03	0.05	0.05	0.08
UO^+	583	367	1300	250	733
UO^+/U^+ (%)	0.1	0.05	0.09	0.08	0.08

[a] Organic solutions contained 500 μg L^{-1} of La and U.

[b] Oxygen was added to the central channel at about 2% of the total aerosol gas flow.

summarizes the data obtained. Sensitivities for La and U varied only slightly among the solvents with the exception of ethanol where the analyte sensitivities are poorer by a factor of 5. The addition of 1-2% O_2 to the central channel while nebulizing ethanol boosts the signal for La^+ and U^+ without a prohibitive increase in the abundance of LaO^+ and UO^+. As expected, acetonitrile gives the lowest MO^+/M^+ ratios since oxygen is not present in this solvent. Metal carbides (MC^+) are not observed for either La (<10 counts s^{-1} net) or U (<20 counts s^{-1} net) in the present work even when the methanol sample contains La and U at 100 mg L^{-1}. The analyte sensitivities obtained from organic solvents are also similar to those observed from aqueous samples with this particular ICP-MS instrument (14, 15).

Organic vs. Inorganic Metal Standards

The objectives of this experiment were to determine a) if inorganic and organic-bound metals had different sensitivities, and b) if volatile and low-melting complexes would be lost in the cryogenic loops. Solutions of inorganic Co, Zn, and Mn ions (e.g., $Zn(NO_3)_2$) at 500 µg L^{-1} were prepared in methanol. A second set of solutions of Co, Zn, and Mn acetates at 500 µg L^{-1} were also prepared in methanol. The melting points for the acetates were measured and are shown in Table 2.

Table 5 shows the measured sensitivities, i.e., count rate per unit concentration. For each metal, the sensitivity from the acetate complex is essentially the same as that from the inorganic nitrate. Thus, little or no analyte is lost from these acetate complexes during the desolvation process. These acetate complexes have melting points of 248°C or higher. They neither melt nor boil in the heaters, which are at 105°C. Thus, the acetate complexes are not volatilized and pass through the desolvation device readily as solid aerosol particles.

Table 5. Sensitivity for analyte elements as acetate complexes and as inorganic nitrate salts in methanol

Element and Isotope	Sensitivity (counts s^{-1} per mg L^{-1})	
	as acetate complex	as nitrate salt
$^{55}Mn^{+}$	$1.6x10^{6}$	$1.7x10^{6}$
$^{59}Co^{+}$	$1.3x10^{6}$	$1.1x10^{6}$
$^{64}Zn^{+}$	$1.1x10^{5}$	$1.4x10^{5}$

Three other metal complexes were tested in the same fashion. Solutions of Co in $Co(CO)_3NO$, 100 μg L^{-1} of Y in $Y(acac)_3$, and 100 μg L^{-1} of Nb in $Nb(OC_2H_5)_5$ were prepared in methanol, with each metal present at 100 μg L^{-1}. Also, solutions of Co, Y, and Nb nitrates at 100 μg L^{-1} were prepared in methanol to serve as reference. As shown in Table 6, the sensitivity for Nb in the low-melting $Nb(OC_2H_5)_5$ is similar to that for the Nb nitrate salt. The sensitivities for Co and Y in the complexes $Co(CO)_3NO$ and $Y(acac)_3$ are actually somewhat higher than the sensitivities for Co and Y as nitrate salts. $Co(CO)_3NO$ boils at 50°C (Table 2), some 55°C below the temperature of the heated loops. Likewise, $Nb(OC_2H_5)_5$ should melt in the heated loops, yet the Nb^+ signal shown in Table 6 for this complex indicates that it passes through the loops readily. Apparently, boiling or melting of the species in these aerosols does not cause a drastic loss of analyte during the desolvation process. Detection limits for Co, Y, and Nb, in either complex or nitrate form, are 80, 20, and 30 ng L^{-1}, respectively.

Memory Effects

Substantial memory effects are seen from some of the complexes, however. The worst such problem is illustrated by the rinse-out curves in Figure 2. The Nb^+ signal when the analyte is present as $Nb(NO_3)_5$ decays to 0.1% of the steady-state level about 60 s after the sample is removed, as noted previously for various elements (14). In contrast, the Nb^+ signal from $Nb(OC_2H_5)_5$ never decays to the 0.1% level but stops at a level corresponding to about 2% of the steady state signal. Similar, though less severe, memory effects are seen for $Y(acac)_3$ and $Co(CO)_3NO$, whose rinse-out curves level off at 0.2% and 0.3% of the steady state signals, respectively.

Table 6. Sensitivity for analyte elements as complexes and as inorganic nitrate salts in methanol

Element and isotope	Sensitivity (counts s^{-1} per mg L^{-1})	
	as complex	as nitrate salt
$^{59}Co^{+}$	2.8×10^{6}[a]	1.7×10^{6}
$^{89}Y^{+}$	3.8×10^{6}[b]	2.4×10^{6}
$^{93}Nb^{+}$	1.8×10^{6}[c]	1.7×10^{6}

[a] Co present as $Co(CO)_3NO$.

[b] Y present as $Y(CH_3COCHCOCH_3)_3$.

[c] Nb present as $Nb(OC_2H_5)_5$.

Memory effects such as this are occasionally seen when solutions containing volatile species are dispersed into finely-divided aerosols. Memory problems can also be exacerbated when the aerosols are heated. For example, inorganic forms of Hg, B, and Os cause similar problems in conventional desolvation systems (18). The precise causes of memory effects are often obscure or not easily attributable to simple chemical reasoning, and the present work is no exception. For example, $Co(CO)_3NO$ boils at 50°C and should be readily volatilized in the heaters, which are at 105°C. $Nb(OC_2H_5)_5$ (b.p. 142°C) should melt in the heaters but not boil, yet $Nb(OC_2H_5)_5$ shows a much worse memory problem than $Co(CO)_3NO$. At any rate, the chemical form of the analyte elements does influence the sample throughput and rinse-out procedures required, as discussed previously by Van Heuzen (16).

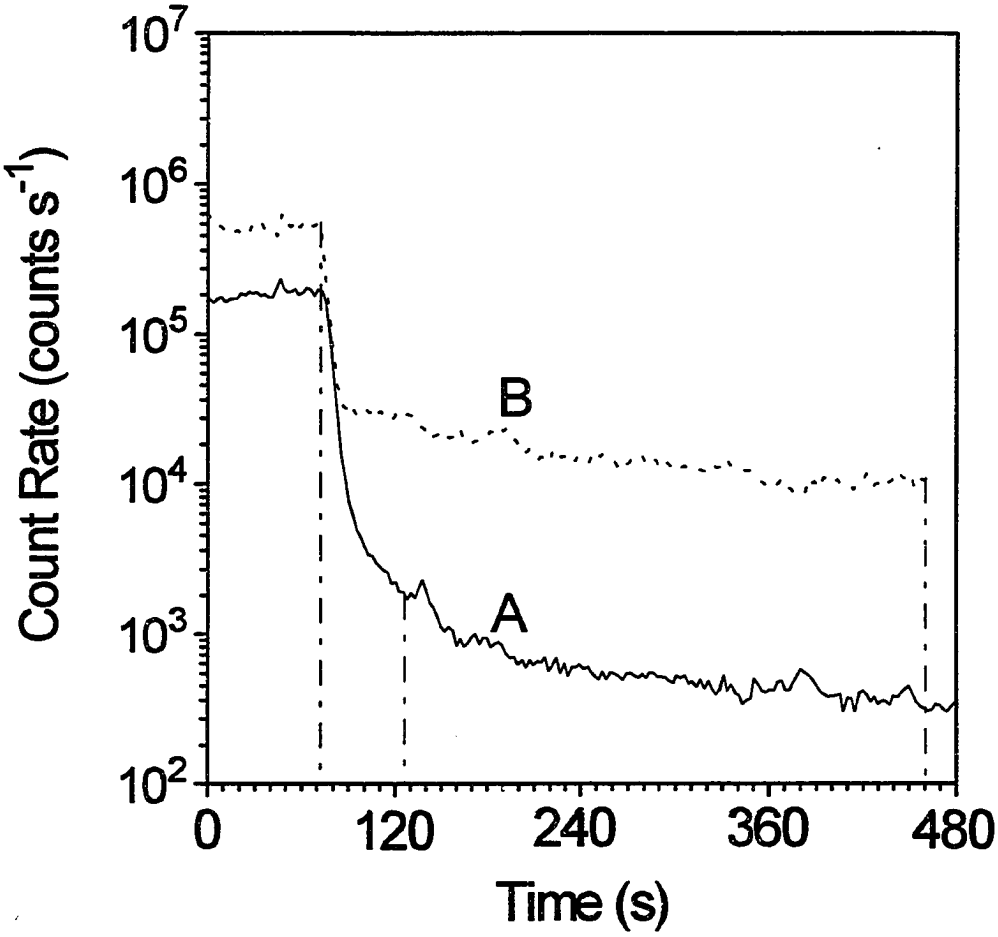

Figure 2. Rinse out curves for Nb^+ in methanol. A: Nb at 100 μg L^{-1} as $Nb(NO_3)_5$; B: Nb at 300 μg L^{-1} as $Nb(OC_2H_5)_5$. In each case, the Nb sample was removed at the time indicated by the vertical dashed line.

CONCLUSION

Cryogenic desolvation allows continuous analysis of difficult solvents that would otherwise plug the sampler or extinguish the plasma. Polyatomic ions are less abundant than is usually the case with organic solvents, although some important analytes are still obscured, particularly ^{28}Si, ^{44}Ca, ^{52}Cr, ^{56}Fe, and ^{68}Zn. This desolvation method should prove valuable for the measurement of trace inorganic ions in highly purified organic solvents used in the semiconductor industry and in materials sciences. However, the analyst should investigate possible memory effects that depend on the chemical form and physical properties of the analyte, particularly when the analyte is present as neutral or volatile complexes. Also, the sensitivity may depend somewhat on the chemical form of the analyte, for reasons that are unclear at this time. In the future, the use of still lower temperatures for the cold loops could prove advantageous, as none of the solvents were frozen into solids in the present work.

ACKNOWLEDGMENTS

The loan of an ultrasonic nebulizer from Cetac Technologies, Inc., is gratefully acknowledged. Ames Laboratory is operated by Iowa State University for the U. S. Department of Energy under Contract No. W-7405-Eng-82. This research was supported by the Office of Basic Energy Sciences, Division of Chemical Sciences.

SAFETY NOTE

Since the heater temperature (100 to 140°C) may be higher than the flash point of the solvent, highly flammable vapors and aerosols produced from organic solvents and organometallic compounds must be kept within the inert gas stream present inside the nebulizer and cryocondensers. The aerosol or vapor must not come in contact with the heating elements on the exterior of the heater. Care should also be observed when handling oxygen. An arrestor valve was installed on the oxygen cylinder.

LITERATURE CITED

(1) Boorn, A. W.; Browner, R. F. *Anal. Chem.* **1982**, *54*, 1402-1410.

(2) Hausler, D. W.; Taylor, L. T. *Anal. Chem.* **1981**, *53*, 1223-1227.

(3) Hausler, D. W.; Taylor, L. T. *Anal. Chem.* **1981**, *53*, 1227-1231.

(4) Kreuning, G.; Maessen, F. J. M. J. *Spectrochim. Acta, Part B* **1989**, *44B*, 367-384.

(5) Maessen, F. J. M. J.; Kreuning, G.; Balke, J. *Spectrochim. Acta, Part B* **1986**, *41B*, 3-25.

(6) Maessen, F. J. M. J.; Seeverens, P. J. H.; Kreuning, G. *Spectrochim. Acta, Part B* **1984**, *39B*, 1171-1180.

(7) Brotherton, T.; Barnes, B.; Vela, N.; Caruso, J. *J. Anal. At. Spectrosc.* **1987**, *2*, 389-396.

(8) Barrett, P.; Pruszkowska, E. *Anal. Chem.* **1984**, *56*, 1927-1930.

(9) Blades, M. W.; Caughlin, B. L. *Spectrochim. Acta, Part B* **1985**, *40B*, 579-591.

(10) Hausler, D. *Spectrochim. Acta, Part B* **1987**, *42B*, 63-73.

(11) Hutton, R. C. *J. Anal. Atomic Spectrom.* **1986**, *1*, 259-263.

(12) Hill, S. J.; Hartley, J.; Ebdon, L. *J. Anal. Atomic Spectrom.* **1986**, *7*, 23-28.

(13) Wiederin, D. R.; Houk, R. S.; Winge, R. K.; D'Silva, A. P. *Anal. Chem.* **1990**, *62*, 1155-1160.

(14) Alves, L. C.; Wiederin, D. R.; Houk, R. S. *Anal. Chem.* **1992**, *64*, 1164-1169.

(15) Alves, L. C.; Allen, L. A.; Houk, R. S. *Anal. Chem.* **1993**, *accepted.*

(16) Van Heuzen, A. A. *4th Surrey Conf. on Plasma Source Mass Spectrom.*, Guildford, UK, July **1991**.

(17) Scott, R. H.; Fassel, V. A.; Kniseley, R. N.; Nixon, D. E. *Anal. Chem.* **1974**, *46*, 75-80.

(18) Fassel, V. A.; Bear, B. R. *Spectrochim. Acta, Part B* **1986**, *41B*, 1089-1113.

(19) Olson, K. W.; Haas, W. J., Jr.; Fassel, V. A. *Anal. Chem.* **1977**, *49*, 632-637.

SUMMARY AND CONCLUSION

The primary purpose of this dissertation has been the development of a desolvation scheme to reduce solvent loading into an ICP. As a consequence of the drastic removal of water and HCl, polyatomic ion interferences (e.g., ClO^+, ArO^+, $ArCl^+$, and MO^+) in ICP-MS were severely diminished (81, 82). The removal of organic solvents permits the determination of trace metals with little or no formation of metal carbides and carbon deposition on the sampling cone when methanol or acetonitrile are used as solvents (83). Two main advantages to the use of cryogenic desolvation with ICP-MS with non-aqueous solutions are: the fact that both the volatile and organometallic compounds tested makes through the cryogenic desolvation apparatus with very little or no analyte loss and the fact that the analyte sensitivities are comparable to the sensitivities observed with aqueous samples with just regular desolvation.

As with any other technique, cryogenic desolvation has its drawbacks and limitations. Cryogenic desolvation is not the panacea for matrix effects. Although Cl^- can be trapped in the cryogenic loops as HCl, the counter cation (usually Na^+ or K^+) reaches the plasma and creates havoc in the determination of trace analytes in a saline matrix. The analyte signal with cryogenic desolvation is only half as much as the signal with regular desolvation. Fortunately, the addition of H_2 to the central channel improves the analyte signal several fold. Only little analyte losses were observed in the cryogenic loops (82) which suggests that the plasma characteristics changed and were responsible for the loss of analyte signal. Substances with high boiling points (e.g., H_2SO_4 330°C) or with very low melting points (e.g., ethanol -117.3°C) are not removed in the cryogenic loops at the temperatures used (+140°C and -80°C). Therefore, not all solvents can be removed by cryogenic desolvation and

solvents such as ethanol and acetone still show too much vapor pressure to be completely removed. The addition of a small dosage of O_2 in addition to cryogenic desolvation seems to be the best solution for analysis of those solvents. Moreover, the considerable memory effects observed when organometallic compounds were present may decrease the sample throughput and deteriorate the detection limits obtainable.

Several possible future experiments employing cryogenic desolvation are imaginable. First, the application of cryogenic desolvation will allow for easy determination of analytes that have been plagued with interferences. Cryogenic desolvation solves many of the spectroscopic overlaps by severely reducing the amount of two of the main elements that form the most troublesome polyatomic ion interferences, oxygen and chlorine.

Second, the increase in analyte signal with the addition of H_2 with cryogenic desolvation is not well understood. The basic reasons for these beneficial effects of H_2 in a dry ICP are intriguing and should be the topic of further study.

There is also room for improvement in the cryogenic hardware. The cryogenic loops currently used are made of copper and gives rise to a substantial copper background when acidic aqueous solutions are used. The obvious answer to this problem is deceptive: use glass. Our efforts with glass loops were unsatisfactory, primarily because glass has a lower thermal conductivity than copper and because the thinnest glass tubing used was still too thick to allow for rapid heat exchange. Glass-lined metal tubings currently on the market also have very thick walls. The solution seems to point towards a thin polymer coating. The most important specifications for the polymer would be high resistance to acids, water, and organic solvents as well as non-porosity to prevent the adsorption of the analyte on the surface. Moreover, it would be advantageous to

use colder temperatures than -80°C since lower vapor pressures for difficult organic solvents could be achieved, and thus further reduce the solvent loading to the plasma. Also, effort should be made to abate the memory effects observed with organometallic compounds.

Finally, the cryogenic desolvation apparatus is straightforward, inexpensive, easy to set up and maintain, and adds little to the learning curve for ICP-MS. It is also easy to switch between cryogenic and regular desolvation and both the plasma and mass spectrometer can be operating at the time. Inertia is a universal physics law that unfortunately also seems to apply in the scientific community whenever a new instrument, technique, or method improvement is brought to surface. It is the opinion of this author that given the time to overcome the inertia, the use of multiple cryogenic desolvation will be seen in the upcoming literature as a means to determine analyte concentrations and isotopes ratios in samples once deemed to arduous and tiresome to tackle with ICP-MS.

ADDITIONAL LITERATURE CITED

(1) Houk, R. S.; Fassel, V. A.; Flesch, G. D.; Svec, H. J.; Gray, A. L.; Taylor, C. E. *Anal. Chem.* **1980**, *52*, 2283-2289.

(2) Gray, A. L.; Date, A. R. *Dynamic Mass Spectrom.* **1981**, *6*, 252-266.

(3) Date, A. R.; Gray, A. L. *Analyst* **1981**, *106*, 1255-1267.

(4) Houk, R. S.; Fassel, V. A.; Svec, H. J. *Dynamic Mass Spectrom.* **1981**, *6*, 234-251.

(5) Date, A. R.; Gray, A. L. *Spectrochim. Acta, Part B* **1983**, *38B*, 29.

(6) Date, A. R.; Gray, A. L. *Analyst* **1983**, *108*, 159.

(7) Gray, A. L.; Date, A. R. *Analyst* **1983**, *108*, 1033.

(8) Douglas, D. J.; Houk, R. S. *Prog. Anal. At. Spectrosc.* **1985**, *8*, 1-18.

(9) Gray, A. L. *Spectrochim. Acta, Part B* **1985**, *40B*, 1525-1537.

(10) Jarvis, K. E.; Gray, A. L.; Houk, R. S. *Handbook of Inductively Coupled Plasma*, 1st ed.; Blackie and Son, London, **1992**.

(11) Houk, R. S. *Anal. Chem.* **1986**, *58*, 97A-105A.

(12) Selby, M.; Hieftje, G. M. *Am. Lab.* **August 1987**, 16-28.

(13) *ICP Inform. Newslet.* **1986**, *12*, 613-619.

(14) Thompson, J. J.; Houk, R. S. *Appl. Spectrosc.* **1987**, *41*, 801-806.

(15) Longerich, H. P.; Strong, D. F.; Kantipuly, C. J. *Can. J. Spectrosc.* **1986**, *31*, 111-121.

(16) Gregoire, D. C. *Anal. Chem.* **1987**, *59*, 2479-2484.

(17) Garbarino, J. R.; Taylor, H. E. *Anal. Chem.* **1987**, *59*, 1568-1575.

(18) Beauchemin, D.; McLaren, J. W.; Berman, S. S. *Spectrochim. Acta, Part B* **1987**, *42B*, 467-490.

(19) Gillson, G. R.; Douglas, D. J.; Fullford, J. E.; Halligan, K. W.; Tanner, S. D. *Anal. Chem.* **1988**, *60*, 1472-1474.

(20) Tan, S. H.; Horlick, G. *J. Anal. At. Spectrom.* **1987**, *2*, 745-763.

(21) Hasegawa, T.; Umemoto, M.; Haraguchi, H.; Hsiech, C.; Montaser, A. in A. Montaser and D. W. Golightly (Eds.), *Inductively Coupled Plasma in Analytical Atomic Spectrometry*, 2nd Edition, VCH, New York, **1992**.

(22) Crain, J. S.; Houk, R. S.; Smith, F. G. *Spectrochim. Acta, Part B* **1988**, *43B*, 1355-1364.

(23) Longerich, H. P. *J. Anal. At. Spectrom.* **1989**, *4*, 665-667.

(24) Gregorie, D. C. *Appl. Spectrosc.* **1987**, *41*, 897-903.

(25) Brotherton, T. J.; Shen, W. -L.; Caruso, J. A. *J. Anal. At. Spectrom.* **1989**, *4*, 39-44.

(26) Wang, J.; Shen, W. -L.; Sheppard, B. S.; Evans, E. H.; Caruso, J. A. *J. Anal. At. Spectrom.* **1990**, *6*, 445-450.

(27) Vickers, G. H.; Ross, B. S.; Hieftje, G. M. *Appl. Spectrosc.* **1989**, *43*, 1330-1333.

(28) Hutton, R. C.; Eaton, A. N. *J. Anal. At. Spectrom.* **1988**, *3*, 547-550.

(29) McLeod, C. W.; Date, A. R.; Cheung, Y. Y. *Spectrochim. Acta, Part B* **1986**, *41B*, 169-174.

(30) Ridout, P. S.; Jones, H. R.; Williams, J. G. *Analyst* **1988**, *113*, 1383-1386.

(31) Vandecasteele, C.; Nagels, M.; Vanhoe, H.; Dams, R. *Anal. Chim. Acta* **1988**, *211*, 91-98.

(32) Hall, G. E. M.; Park, C. J.; Pelchat, J. C. *J. Anal. Atom. Spectrom.* **1987**, *2*, 189-196.

(33) Gregorie, D. C. *Spectrochim. Acta, Part B* **1987**, *42B*, 895-907.

(34) Gregorie, D. C. *Pap. -Geol. Surv. Can.* **1986**, *86-1B*, 39-45.

(35) Boomer, D. W.; Powell, M. J. *Can. J. Spectrosc.* **1986**, *31*, 104-109.

(36) Ting, B. T. G.; Janghorbani, M. *Spectrochim. Acta, Part B* **1987**, *42B*, 21-28.

(37) Wiederin, D. R.; Smyczek, R. E.; Houk, R. S. *Anal. Chem.* **1991**, *63*, 1626-1631.

(38) Palmieri, M. D.; Fritz, J. S.; Thompson, J. J.; Houk, R. S. *Anal. Chim. Acta* **1986**, *184*, 187-196.

(39) Jiang, S. -J.; Palmieri, M. D.; Fritz, J. S.; Houk, R. S. *Anal. Chim. Acta* **1987**, *200*, 559-571.

(40) Beauchemin, D.; McLaren, J. W.; Mykytiuk, A. P.; Berman, S. S. *Anal. Chem.* **1987**, *59*, 778-783.

(41) Beauchemin, D.; McLaren, J. W.; Mykytiuk, A. P.; Berman, S. S. *Anal. Chem.* **1988**, *60*, 687-691.

(42) Beauchemin, D.; McLaren, J. W.; Mykytiuk, A. P.; Berman, S. S. *J. Anal. Atom. Spectrom.* **1988**, *3*, 305-308.

(43) McLaren, J. W.; Mykytiuk, A. P.; Willie, S. N.; Berman, S. S. *Anal. Chem.* **1985**, *57*, 2907-2911.

(44) Plantz, M. R.; Fritz, J. S.; Smith, F. G.; Houk, R. S. *Anal. Chem.* **1989**, *61*, 149-153.

(45) Gray, A. L. *Spectrochim. Acta, Part B* **1986**, *41B*, 151-167.

(46) Vaughan, M.-A.; Horlick, G. *Appl. Spectrosc.* **1986**, *40*, 434-445.

(47) Tan, S. H.; Horlick, G. *Appl. Spectrosc.* **1986**, *40*, 445-460.

(48) Vaughan, M. A.; Horlick, G. *Appl. Spectrosc.* **1987**, *41*, 523-526.

(49) Gray, A. L.; Williams, J. G. *J. Anal. At. Spectrom.* **1987**, *2*, 599-606.

(50) Date, A. R.; Cheung, Y. Y.; Stuart, M. E. *Spectrochim. Acta, Part B* **1987**, *42B*, 3-20.

(51) Gray, A. L.; Williams, J. G. *J. Anal. At. Spectrom.* **1987**, *2*, 81-82.

(52) Kubota, M.; Fudagawa, N.; Kawase *A. Anal. Sci. (Japan)* **1989**, *5*, 701-706.

(53) Lichte, F. E.; Meier, A. L.; Crock, J. G. *Anal. Chem.* **1987**, *59*, 1150-1157.

(54) Doherty, W.; Vander Voet, A. *Can. J. Spectrosc.* **1985**, *30*, 135-141.

(55) McLaren, J. W.; Beauchemin, D.; Berman, S. S. *Anal. Chem.* **1987**, *59*, 610-613.

(56) Horlick, G.; Tan, S. H.; Vaughan, M. A.; Rose, C. A. *Spectrochim. Acta, Part B* **1985**, *40B*, 1555-1572.

(57) Vaughan, M.-A.; Horlick, G.; Tan, S. H. *J. Anal. Atom. Spectrom.* **1987**, *2*, 765-772.

(58) Gray, A. L.; Houk, R. S.; Williams, J. G. *J. Anal. Atom. Spectrom.* **1987**, *2*, 13-20.

(59) Olivares, J. A.; Houk, R. S. *Anal. Chem.* **1985**, *57*, 2674-2679.

(60) Long, S. E.; Brown, R. M. *Analyst* **1986**, *111*, 901-906.

(61) Zhu, G.; Browner, R. F. *Appl. Spectrosc.* **1987**, *41*, 349-359.

(62) Longerich, H. P.; Fryer, B. J.; Strong, D. F.; Kantipuly, C. J. *Spectrochim. Acta, Part B* **1987**, *42B*, 75-92.

(63) Ebdon, L.; Evans, E. H.; Barnett, N. W. *J. Anal. At. Spectrom.* **1989**, *4*, 505-508.

(64) Hutton, R. C. *J. Anal. At. Spectrom.* **1986**, *1*, 259-263.

(65) Barret, P.; Pruszkowska, E. *Anal. Chem.* **1984**, *56*, 1927-1930.

(66) Nygaard, D. D.; Schleicher, R. G.; Sotera, J. J. *Appl. Spectrosc.* **1986**, *40*, 1074.

(67) Boorn, A. W.; Browner, R. F. *Anal. Chem.* **1982**, *54*, 1402-1410.

(68) Aldeo, J. D.; Heine, D. R.; Philips, H. A.; Hoek, F. B. G.; Schneide, M. R.; Freelin, J. M.; Denton, M. B. *Spectrochim. Acta, Part B* **1983**, *40B*, 1447.

(69) Brown, R. J. *Spectrochim. Acta, Part B* **1983**, *38B*, 283.

(70) Gast, C. H.; Kraak, J. C.; Poppe, H.; Maessen, F. J. M. J. *J. Chromatogr.* **1979**, *185*, 549.

(71) Maessen, F. J. M. J.; Kreuning, G.; Balke, J. *Spectrochim. Acta, Part B* **1986**, *41B*, 3-25.

(72) Kreuning, G.; Maessen, F. J. M. J. *Spectrochim. Acta, Part B* **1987**, *42B*, 677-688.

(73) Nygaard, D. D.; Sotera, J. J. *Appl. Spectrosc.* **1987**, *41*, 703-704.

(74) Maessen, F. J. M. J.; Seeverens, P. J. H.; Kreuning, G. *Spectrochim. Acta, Part B* **1984**, *39B*, 1171-1180.

(75) Kreuning, G.; Maessen, F. J. M. J. *Spectrochim. Acta, Part B* **1989**, *44B*, 367-384.

(76) Hausler, D. W.; Taylor, L. T. *Anal. Chem.* **1981**, *53*, 1227-1231.

(77) Hausler, D. W.; Taylor, L. T. *Anal. Chem.* **1981**, *53*, 1223-1227.

(78) Hausler, D. W. *Spectrochim. Acta, Part B* **1987**, *42B*, 63-73.

(79) Hill, S. J.; Hartley, J.; Ebdon, L. *J. Anal. At. Spectrom.* **1992**, *7*, 895-898.

(80) Hill, S. J.; Hartley, J.; Ebdon, L. *J. Anal. At. Spectrom.* **1992**, *7*, 23-28.

(81) Alves, L. C.; Wiederin, D. R.; Houk, R. S. *Anal. Chem.* **1992**, *64*, 1164-1169.

(82) Alves, L. C.; Allen, L. A.; Houk, R. S. *Anal. Chem.* **1993**, *accepted.*

(83) Alves, L. C.; Minnich, M. G.; Wiederin, D. R.; Houk, R. S. *J. Anal. At. Spectrom.* **1993**, *submitted.*

ACKNOWLEDGMENTS

First, I would like thank God for being my guiding light and strength all my life. Also, I have to thank Him for my family and friends to whom I am greatly indebted. I would like to take the next few lines to express my gratitude to them.

I owe much of what I know to the people that have taken upon them the task of educating me. I would like to thank my major professor, R. S. Houk (Sam) for sharing with me his tremendous knowledge and expertise in ICP-MS and analytical chemistry. I sincerely appreciate his guidance and patience towards me and I thank him for teaching me self-initiative, motivation, and analytical thinking.

I would like to express my appreciation to Dr. Dennis Johnson and Dr. Marc Porter for their friendship and support. I must also acknowledge all my professors from Escola Técnica Federal de Química do Rio de Janeiro. They were the first ones to instill in me the love for chemistry. I would like to show my gratitude to Universidade Estadual do Rio de Janeiro (UERJ) and Carthage College for giving me a solid background and for inspiring me to continue my education at Iowa State University.

I would like to thank Ames Laboratory, Iowa State University, and the U. S. Department of Energy for funding. Likewise, if it wasn't for the Institute Brazil–United States (IBEU) and the Fullbright Scholarship, I couldn't have afforded to come to the United States for my undergraduate. I hope IBEU and Fullbright will be able to continue their invaluable work for many years to come. I strongly advocate others to experience a different culture from their own. It is quite an eye opener and you truly come to respect and admire people's differences and opinions. There's no place for any form of discrimination or racism in the world.

Ames Laboratory was an extension of my home. I spent many an hour there and I had the opportunity to meet many people and make many friends. I would like to acknowledge the Machine Shop, the Electronic, and Computer groups. I would especially like to thank Marlene Frisk and John Homer for teaching me a lot about computers. I would like to acknowledge the Houk Group, past and present members alike, for their support, cooperation, and friendship. I would especially like to thank Daniel Wiederin for getting me started on cryogenic desolvation. I would also like to thank Lloyd Allen and Mike Minnich for working with me on two of my projects. I wish you both success in your graduate school experience.

The friends I made while in Kenosha (Wisconsin) have a special place in my heart. They were my first friends in the U. S. and I will always love them. They did their best to understand me at the time in my life when I truly could not express my feelings and thoughts very well. They are all my friends from Carthage College and the First Presbyterian Church. I would especially like to thank three families: the Carvalhos (my only link to Portuguese in Kenosha), the Levys (my very first American contact and friends), and the Van Dahms (my one and only American "Muffin" parents!). I could not have survived my first years in the U. S. without your generosity and friendship.

Likewise, I would like to thank Viviane dos Santos for being such a good friend and pen pal (ETFQ-RJ forever!) and Rose Turano for preparing me well to my coming to the United States. The "cultural shock" and homesickness were a lot more bearable thanks to you.

I would like to express my profound gratitude to my wife for her companionship, friendship, and support. I would also like to thank the Cihals (my in-laws) for accepting me into their family with open arms.

My Brazilian family means a lot to me. I never realized how much I loved them until I came to United States. I am an extension of them and they will always be with me wherever I am. I wish you all the best and I have you constantly in my prayers.

Last, but definitely not least, I would like to thank three special ladies that have shared in my life, loved me unconditionally, and helped me no matter how far I was from them: my Mom Eunice, my godmother Zilda, and my grandma Ruth. I couldn't have accomplished anything without you. You went through many sacrifices, and I know at times you have gone without so I would not have to. You have always supported me in my endeavors, believed in me, and urged me to do my best. You have been my drive and inspiration, my support and my hope. I owe you my greatest debt and I will have you forever in my heart. To you I say, simply, very simply, with immense gratitude, "Muito Obrigado !"

APPENDIX

Potential interferences in ICP-MS. This listing was compiled by Luis Alves from the available literature.

1
H (99.985%)

2
H (0.015%)

3
He
(0.00014%)

4
He
(99.99986%)

6
Li (7.5%)

7
Li (92.5%)

9
Be (100%)

10
B (19.8%)

11
B (80.2%)

12
C (98.90%)

13
C (1.10%)

14
N (99.63%)
CH_2

15
N (0.37%)
NH
CH_3

16
O (99.762%)
NH_2
CH_4

17
O (0.038%)
OH
NH_3

18
O (0.200%)
H_2O

19
F (100%)
H_3O

20
Ne (90.51%)
Ca^{+2}

21
Ne (0.21%)
Ca^{+2}

22
Ne (9.22%)
Ca^{+2}

23
Na (100%)
Ca^{+2}

24
Mg
(78.99%)
C_2
Ca^{+2}

25
Mg
(10.00%)
C_2H

26
Mg
(11.01%)
CN
C_2H_2

27
Al (100%)
HCN
C_2H_3

28
Si (92.23%)
N_2
CO
CH_2N
C_2H_4

29
Si (4.67%)
HN_2
CHO
CH_3N
C_2H_5

30
Si (3.10%)
NO
H_2N_2
CH_2O
CH_4N
C_2H_6

31

P (100%)
HNO
H_3N_2
CH_3O
CH_5N

32

S (95.02%)
O_2

33

S (0.75%)
O_2H

34

S (4.21%)
$^{16}O^{18}O$

35

Cl (75.77%)

36

S (0.02%)
Ar (0.337%)

37

Cl (24.23%)
^{36}ArH

38

Ar (0.063%)

39

K
(93.2581%)
^{38}ArH

40

Ar (99.60%)
K (0.0117%)
Ca
(96.941%)
MgO

41

K (6.7302%)
^{40}ArH
MgO

42

Ca (0.647%)
MgO
Sr^{+2}

43

Ca (0.135%)
Sr^{+2}

44

Ca (2.086%)
CO_2
Sr^{+2}

45

Sc (100%)
CO_2H

46

Ca (0.004%)
Ti (8.0%)
NO_2
^{32}SN

47

Ti (7.3%)
PO

48

Ca (0.187%)
Ti (73.8%)
^{32}SO
POH

49

Ti (5.5%)
^{32}SOH
ClN
^{33}SO

50

Ti (5.4%)
V (0.25%)
Cr (4.35%)
^{34}SO

51

V (99.75%)
^{35}ClO
^{34}SOH

52

Cr (83.79%)
ArC
^{36}ArO
$^{35}ClOH$

53

Cr (9.50%)
^{37}ClO

54

Cr (2.36%)
Fe (5.8%)
ArN
$^{37}ClOH$

55

Mn (100%)
ArNH

56

Fe (91.72%)
ArO
CaO

57

Fe (2.2%)
ArOH

58

Fe (0.28%)
Ni (68.27%)
$^{40}Ar^{18}O$
CaO

59

Co (100%)
CaO

60

Ni (26.10%)
CaO

61

Ni (1.13%)
ScO

62

Ni (3.59%)
CaO, TiO

63

Cu (69.17%)
ArNa
TiO, PO_2

64

Ni (0.91%)
Zn (48.6%)
$^{32}SO_2$
$^{32}S_2$
ArC_2
TiO, CaO

65

Cu (30.83%)
$^{32}SO_2H$
TiO
Ba^{+2}

66

Zn (27.9%)
$^{34}SO_2H$
TiO, VO,
CrO
Ba^{+2}

67

Zn (4.1%)
$^{35}ClO_2$
VO
Ba^{+2}

68

Zn (18.8%)
$^{40}ArN_2$
CrO
Ba^{+2}, Ce^{+2}

69

Ga (60.1%)
$^{37}ClO_2$
CrO
Ba^{+2}, Ce^{+2},
La^{+2}

70

Zn (0.6%)
Ge (20.5%)
$^{40}ArNO$
$^{35}Cl_2$
CrO
Ce^{+2}, Nd^{+2}

71

Ga (39.9%)
ArP
Ce^{+2}, Nd^{+2}

72

Ge (27.4%)
K (83.80%)
$^{40}Ar^{32}S$
$^{35}Cl^{37}Cl$
Nd^{+2},
Sm^{+2}

73

Ge (7.8%)
Nd^{+2}

74

Ge (36.5%)
Se (0.9%)
$^{40}Ar^{34}S$
$^{37}Cl_2$
Nd^{+2},
Sm^{+2}

75

As (100%)
$Ar^{35}Cl$
Nd^{+2},
Sm^{+2}

76

Ge (7.8%)
Se (9.0%)
$^{40}Ar^{36}Ar$
Sm^{+2}, Gd^{+2}

77

Se (7.6%)
$Ar^{37}Cl$
Sm^{+2}, Gd^{+2}

78

Se (23.5%)
K (0.35%)
$^{40}Ar^{38}Ar$
Gd^{+2}, Dy^{+2}

79

Br (50.69%)
ArK
Gd^{+2}, Dy^{+2}

80

Se (49.6%)
K (2.25%)
$^{40}Ar_2$
ArCa
Gd^{+2}, Dy^{+2}

81

Br (49.31%)
$^{40}Ar_2H$
Dy^{+2}, Er^{+2}

82

Se (9.4%)
K (11.6%)
Dy^{+2}, Er^{+2}

83

K (11.5%)
Er^{+2}

84

K (57.0%)
Sr (0.56%)
Er^{+2}, Yb^{+2}

85

Rb (72.17%)
Er^{+2}, Yb^{+2}

86

K (17.3%)
Sr (9.86%)
Yb^{+2}

87

Rb (27.83%)
Sr (7.00%)
Yb^{+2}

88

Sr (82.58%)
Yb^{+2}, Lu^{+2}

89

Y (100%)

90

Zr (51.45%)

91

Zr (11.27%)

92

Zr (17.17%)
Mo
(14.84%)

93

Nb (100%)

94
Zr (17.33%)
Mo (9.5%)

95
Mo
(15.92%)

96
Zr (2.78%)
Mo
(16.68%)
Ru (5.52%)

97
Mo (9.55%)

98
Mo
(24.13%)
Ru (1.88%)

99
Ru (12.7%)

100
Mo (9.63%)
Ru (12.6%)
SrO

101
Ru (17.0%)
SrOH

102
Ru (31.6%)
Pd (1.02%)
SrO

103
Rh (100%)
SrO
SrOH

104
Ru (18.7%)
Pd (11.14%)
SrO
SrOH

105
Pd (22.33%)
SrOH
YO

106
Pd
(+27.33%)
Cd (1.25%)
ZrO

107
Ag (51.84%)
ZrO

108
Pd (26.46%)
Cd (0.89%)
ZrO, MoO

109
Ag (48.16%)
ZrO, MoO,
NbO

110
Pd (11.72%)
Cd (12.49%)
ZrO, MoO

111
Cd (12.80%)
ZrO, MoO

112
Cd (24.13%)
Sn (1.0%)
ZrO, MoO

113
Cd (12.22%)
In (4.3%)
MoO

114
Cd (28.73%)
Sn (0.7%)
MoO

115
Sn (0.4%)
In (95.7%)
MoO

116
Cd (7.49%)
Sn (14.7%)
MoO

117
Sn (7.7%)
U^{+2}

118
Sn (24.3%)

119
Sn (8.6%)
U^{+2}

120
Sn (32.4%)
Te (0.096%)

121
Sb (57.3%)

122
Sn (4.6%)
Te (2.60%)

123
Sb (42.7%)
Te (0.903%)

124
Sn (5.66%)
Te (4.816%)
Xe (0.10%)

125
Te (7.14%)

126
Te (18.95%)
Xe (0.09%)

127
I (100%)

128
Te (31.69%)
Xe (1.91%)

129
Xe (26.4%)

130
Te (33.80%)
Xe (4.1%)
Ba (0.106%)

131
Xe (21.2%)

132
Xe (26.9%)
Ba (0.101%)

133
Cs (100%)

134
Ba (2.417%)

135
Ba (6.592%)

136
Xe (8.9%)
Ba (7.854%)
Ce (0.19%)

137
Ba (11.23%)

138
Ba (71.70%)
La (0.09%)
Ce(0.25%)

139
La (99.91%)

140
Ce (88.48%)

141
Pr (100%)

142
Ce (11.08%)
Nd (27.13%)

143
Nd (12.18%)

144
Nd (23.80%)
Sm (3.1%)

145
Nd (8.30%)

146
Nd (17.19%)
BaO

147
Sm (15.0%)
BaOH

148
Nd (5.76%)
Sm (11.3%)
BaO

149
Sm (13.8%)
BaOH

150
Nd (5.64%)
Sm (7.4%)
BaO

151
Eu (47.8%)
BaO
BaOH

152
Sm (26.7%)
Gd (0.20%)
BaO, CeO
BaOH

153
Eu (52.2%)
BaO
BaOH

154
Sm (22.7%)
Gd (2.18%)
BaOH
CeO, BaO, LaO

155
Gd (14.80%)
BaOH
LaO

156
Gd (20.47%)
Dy (0.06%)
CeO

157
Gd (15.65%)
PrO

158
Gd (24.84%)
Dy (0.10%)
CeO, NdO

159
Tb (100%)
NdO

160
Gd (21.86%)
Dy (2.34%)
NdO, SmO

161
Dy (18.9%)
NdO

162
Dy (25.5%)
Er (0.14%)
NdO

163
Dy (24.9%)
NdO, SmO

164
Dy (28.2%)
Er (1.61%)
NdO, SmO

165
Ho (100%)
SmO

166
Er (33.6%)
NdO, SmO

167
Er (22.95%)
EuO

168
Er (26.8%)
Yb (0.13%)
SmO, GdO

169
Tm (100%)
EuO

170
Er (14.9%)
Yb (3.05%)
SmO, GdO

171
Yb (14.3%)
GdO

172
Yb (21.9%)
GdO, DyO

173
Yb (16.12%)
GdO

174
Yb (31.8%)
Hf (0.16%)
GdO, DyO

175
Lu (97.40%)
TbO

176
Yb (12.7%)
Lu (2.59%)
Hf (5.2%)
GdO, DyO

177
Hf (18.6%)
DyO

178
Hf (27.1%)
DyO, ErO

179
Hf (13.74%)
DyO

180
Hf (35.2%)
Ta (0.012%)
W (0.13%)
DyO, ErO

181
Ta
(99.998%)
HoO

182
W (26.3%)
ErO

183
W (14.3%)
ErO

184
W (30.67%)
Os (0.02%)
ErO, YbO

185
Re (37.40%)
TmO

186
W (28.6%)
Os (1.58%)
ErO, YbO

187
Re (62.6%)
Os (1.6%)
YbO

188
Os (13.3%)
YbO

189
Os (16.1%)
YbO

190
Os (26.4%)
Pt (0.01%)
YbO, HfO

191
Ir (37.3%)
LuO

192
Os (41.0%)
Pt (0.79%)
YbO, HfO, LuO

193
Ir (62.7%)
HfO

194
Pt (32.9%)
HfO

195
Pt (33.8%)
HfO

196
Pt (25.3%)
Hg (0.15%)
HfO, TaO, WO

197
Au (100%)
TaO

198
Pt (7.2%)
Hg (10.1%)
WO

199
Hg (17%)
WO

200
Hg (23.1%)
WO

201
Hg (13.2%)

202
Hg (29.65%)
WO

203
Tl (29.52%)

204
Hg (6.8%)
Pb (1.4%)

205
Tl (70.476%)

206
Pb (24.1%)

207
Pb (22.1%)

208
Pb (52.4%)

209
Bi (100%)

230
Pa (100%)

232

Th (100%)

234

U (0.0054%)

235

U (0.7110%)

238

U

(99.2830%)

248

ThO

250

UO

251

UO

254

UO